

Review

# Scientific Challenges and Present Capabilities in Underwater Robotic Vehicle Design and Navigation for Oceanographic Exploration Under-Ice

Laughlin D. L. Barker <sup>1,2</sup>, Michael V. Jakuba <sup>3</sup>, Andrew D. Bowen <sup>3</sup>, Christopher R. German <sup>4</sup>, Ted Maksym <sup>3</sup>, Larry Mayer <sup>4,5</sup>, Antje Boetius <sup>6</sup>, Pierre Dutrieux <sup>7,8</sup> and Louis L. Whitcomb <sup>1,3,\*</sup>

<sup>1</sup> Department of Mechanical Engineering, Johns Hopkins University, Baltimore, MD 21218, USA; laughlinbarker@gmail.com

<sup>2</sup> Department of Marine Operations, Monterey Bay Aquarium Research Institute, Moss Landing, CA 95039, USA

<sup>3</sup> Department of Applied Ocean Physics and Engineering, Woods Hole Oceanographic Institution, Woods Hole, MA 02543, USA; mjakuba@whoi.edu (M.V.J.); abowen@whoi.edu (A.D.B.); tmaksym@whoi.edu (T.M.)

<sup>4</sup> Department of Geology and Geophysics, Woods Hole Oceanographic Institution, Woods Hole, MA 02543, USA; cgerman@whoi.edu (C.R.G.); larry@ccom.unh.edu (L.M.)

<sup>5</sup> Center for Coastal and Ocean Mapping/Joint Hydrographic Center, University of New Hampshire, Durham, NH 03824, USA

<sup>6</sup> Alfred Wegener Institute, Helmholtz Centre for Polar and Marine Research, 27570 Bremerhaven, Germany; Antje.Boetius@awi.de

<sup>7</sup> Lamont-Doherty Earth Observatory, Columbia University, Palisades, NY 10964, USA; pierred@ldeo.columbia.edu

<sup>8</sup> British Antarctic Survey, Cambridge CB3 0ET, UK

\* Correspondence: llw@jhu.edu

Received: 30 June 2020; Accepted: 6 August 2020; Published: 11 August 2020



**Abstract:** This paper reviews the scientific motivation and challenges, development, and use of underwater robotic vehicles designed for use in ice-covered waters, with special attention paid to the navigation systems employed for under-ice deployments. Scientific needs for routine access under fixed and moving ice by underwater robotic vehicles are reviewed in the contexts of geology and geophysics, biology, sea ice and climate, ice shelves, and seafloor mapping. The challenges of under-ice vehicle design and navigation are summarized. The paper reviews all known under-ice robotic vehicles and their associated navigation systems, categorizing them by vehicle type (tethered, untethered, hybrid, and glider) and by the type of ice they were designed for (fixed glacial or sea ice and moving sea ice).

**Keywords:** underwater robotic vehicles; under-ice navigation; tethered vehicles; hybrid vehicles; gliders; ocean science; ocean exploration

## 1. Introduction

This paper seeks to review the scientific motivation, challenges, development, and use of underwater robotic vehicles designed for diving in ice-covered waters, with special attention paid to the navigation systems employed for under-ice deployments. The world's oceans cover 71% of the Earth's surface, 12% of which is largely inaccessible to scientific research due to being covered by ice all or part of the year. In the Northern Hemisphere, sea ice coverage varies seasonally from 102%

to 192% the size of the United States, and in the Southern Hemisphere sea ice coverage varies seasonally from 39% to 260% the size of Australia (equivalently 30% to 205% the size of the United States) [1].

Few methods presently exist for routine deep water and benthic survey and sampling operations under ice in high latitudes. In contrast, present day blue-water oceanographic methods for survey and sampling are extensive—they include ship-based sensing; lowered and towed instruments such as dredges, Conductivity Temperature Depth (CTD) instruments, and deep-tows tethered Remotely Operated Vehicles (ROVs); and untethered vehicles such as Human Occupied Vehicles (HOVs), Autonomous Underwater Vehicles (AUVs), and Hybrid Remotely Operated Vehicles (HROVs). Only a few of these methods, principally vertically lowered instruments deployed from icebreaking ships, e.g., in [2], or from ice camps, e.g., in [3], are regularly practiced for under-ice sampling and survey operations. It remains difficult to effectively employ most open water methods in ice-covered high-latitude seas because of the constrained maneuverability inherent in icebreaker operations. Over-the-side deployments of lowered instruments generally prohibit ice-breaking and constrain the ship to the wind-driven motion of the ice. Even then, drifting sea ice is a threat to the cables used to deploy the instrumentation. The first reported attempts of scientific observation beneath ice-covered waters involved depth and hydrographic measurements (Nansen's 1893–1896 *Fram* Expedition [4]) and, in the 20th century, the analysis of sonar measurements and officer's cruise reports from military submarine missions dating back to the 1950s [5]. Even in the present day, large parts of polar seafloor remain uncharted [6,7]. Hydrographic mesoscale structures and processes, like ocean fronts and eddies, upwelling, and downwelling, requiring 3D surveys by AUVs are extremely difficult to realize under the ice [8,9]. Likewise, the discovery and observation of polar life, which contains a high proportion of endemic species, remains an important task [10]. Very little is known about the specific adaptations of polar life to its extreme habitat. Understanding these is critical in the face of rapid climate change and sea ice decline [11].

New methods for surveying and sampling under permanent moving sea ice are needed to address a range of critically important geologic, biologic, geochemical, oceanographic, and climatic problems. For example, ultra-slow Mid-Ocean Ridges (MORs) occur in geographic regions where weather windows are extremely narrow or there is ice cover (e.g., the Southwest Indian Ridge and the Gakkel Ridge). With the recent identification of hydrothermal vents during first-order mapping studies of these ultra-slow spreading ridges [2,12–15], scientists are poised to make breakthroughs in our understanding of this important end-member of the sea floor spreading environment. The ability to sample and observe detailed geological, biological, and chemical processes occurring at the slowest spreading MORs could revolutionize our understanding of how sea floor spreading is manifested in these settings. In addition, a host of new and novel biological communities and chemical/biochemical processes may be associated with ultra-slow spreading MORs.

New methods for surveying and sampling under glacial ice shelves are needed to provide scientific access to the water column, sea floor, grounding line, and underside of the ice shelves, which remain among the least explored frontiers worldwide. These cavities under ice shelves host poorly understood processes that control most of the global sea level uncertainty over the next decades to century [16]. A preliminary draft of Sections 3–5 of this paper appeared in [17].

The remainder of this paper is organized as follows. Section 2 reviews the scientific motivation and challenges for remote under-ice oceanographic exploration, addressing these issues in the scientific contexts of geology and geophysics, biology, sea ice and climate, ice shelves, and seafloor mapping. Section 3 briefly reviews several approaches to vehicle navigation under ice. Section 4 reviews previously reported vehicle systems designed for use under fixed ice—landfast sea ice or ice shelves. Section 5 reviews previously reported vehicle systems designed for use under moving sea ice. Section 6 summarizes and concludes.

## 2. Scientific Motivation and Challenges for Remote Under-Ice Oceanographic Exploration

This section reviews the scientific motivation and challenges for remote under-ice oceanographic exploration, addressing these issues in the following scientific contexts; Ice Shelves (Section 2.1), Sea Ice and Ocean (Section 2.2), Biology (Section 2.3), Seafloor Mapping (Section 2.4), and Geology and Geophysics (Section 2.5).

### 2.1. Ice Shelves

A part of the world where climate changes are the largest and the most iconic is the poles, where the Greenland and Antarctic ice sheets meet continental shelf seas. In the Arctic, atmospheric warming and other processes are leading to a shrinking ice sheet, increased subglacial runoff and the associated amplified interaction with the ocean [18], and weakening of the ice sheet buttressing glacial margins [19,20], with important implication to global sea level [21]. In the Antarctic, both atmospheric (Antarctic Peninsula) and ocean-driven melting (West Antarctica) of the ice shelves conspire to accelerate the flow of land ice into the ocean [16], thereby contributing significantly to sea level rise [22], and freshening continental shelf seas and the Southern Ocean [23,24]. In addition to sea level concerns, ice sheet–ocean interactions in Antarctica are key to the formation of dense waters that fill to global oceans abyss [25], and the melt-driven upwelling arising from the freshening and associated buoyancy gain is also thought to provide crucial nutrients for primary production in Southern continental shelf seas [26,27], with consequential contribution to the global biological carbon pump [28].

Around most of Greenland, the interaction between the ice and the ocean happens along a one to tens of kilometers wide, hundreds of meters high vertical ice face that flows into a fjord setting. Around most of Antarctica, the interaction mostly arises under an ice shelf, the floating extension of grounded glacial ice, within an ocean cavity covering tens to hundreds of kilometers in the horizontal and hundreds of meters in the vertical. These scales align rather well with present autonomous underwater vehicle capabilities, and remarkable progress in our understanding has been achieved thanks to few but precious forays into these treacherous environments.

The deployment of Autosub2 under the Fimbul ice shelf in East Antarctica showed a complex, irregular ice base geometry [29]. A few years later, the extensive observations under Pine Island Glacier ice shelf in West Antarctica revealed the importance of seabed bathymetry in shaping the access of the warmest deepest waters to the most sensitive glacier grounding line [30], the glacial retreat history [31], the glacial melt sensitivity to oceanic variability [32], and the broader connections with climate variability [33,34]. The same missions also imaged important features on the seabed [35,36] and the ice base [37,38]. The latter, instead of the irregular features discerned earlier, is organized in a series of kilometer-wide, hundred meter high channels that drive the circulation and heat exchange at the ice–ocean interface, and are also carved by melt [39,40]. In turn, the flanks of such channels are not smooth, but instead harbor a terraced geometry that is also carved by and modulates melting [37], hinting at a tightly coupled ice–ocean system.

These advances led to new AUV operations, first repeating surveys under Pine Island Glacier ice shelf with modified sensor payload [41] and more recently exploring other settings, expanding the diversity of vehicle types and capabilities (see Section 4).

### 2.2. Sea Ice and Ocean

The decline of Arctic sea ice is one of the most conspicuous examples of climate change; September ice extent is now ~35% lower than four decades ago. In contrast, Antarctic sea ice extent has increased modestly over the same period, only to drop to record lows in 2016 from which it has yet to fully recover [42]. Neither of these trends are adequately captured by models [43,44]. In the Arctic, sea ice has also thinned dramatically, with the loss of almost all ice more than a few years old [42]. Thinning was first established between the late 1950s–1979 and the 1990s from extensive upward-looking sonar from

American and British submarines [45,46], a trend that has continued to be observed by satellites [47,48]. Under-ice vehicles have the advantage of an unobstructed view of the ice underside. Equipped with multibeam sonar, they can provide a detailed view of ice morphology and understanding of the mechanical thickening driven by ice dynamics that is otherwise very challenging to measure, particularly for thicker, ridged ice [49,50]. Because only a small fraction of sea ice rises above sea level, and is usually concealed under a layer of snow, sonar measurements of the ice draft provide the most reliable estimate of sea ice thickness. Such observations can help validate satellite altimeter estimates of sea ice thickness [51], particularly at the high spatial resolutions possible with the recently launched ICESAT-2 [52].

Sea ice change is closely coupled with changes in the upper ocean. The Arctic maintains a perennial ice cover in part because it is insulated from the heat of warmer waters at depth by cold, fresher surface waters. This stratification results from a complex series of pathways and physical mechanisms, including inflows of both warm and cold Pacific-sourced waters at shallow depths, a warm inflow of Atlantic Water at intermediate depths, riverine input, sea ice melt and growth, and solar heating, that are not well observed or understood (see, e.g., in [53]). In the Eastern Arctic, increasing inflow and temperature of Atlantic Water has been observed, contributing to reduced ice growth in winter [54]. In the Western Arctic, the increasingly seasonal ice cover has been accompanied by increased inflow of warm Pacific water through the Bering Strait, thought to contribute to reduced summer ice extent and potentially winter ice growth [55], increased solar heating at shallow depths that retards autumn ice growth, and may also act as a source of heat to limit winter ice growth [56,57]. While strong stratification presently limits the role of the latter, this may increase alongside the observed increase in the role of waves and storms [58] and a thinner, more mobile ice cover.

Of particular interest to vehicle operations beneath the Arctic ice cover is the development of the “Beaufort lens”, a sound duct that forms as cooler Pacific Winter Water is sandwiched between warm Pacific Summer Water at depths of 50–100 m and warm, salty layer of Atlantic sourced waters at depths below 150–200 m. Regionally and seasonally variable, this sound duct can enable acoustic communication over distances up to 400 km [59].

In the Antarctic, a thin, seasonal ice cover is maintained in part by the weak upper ocean stratification that facilitates stronger ice–ocean interactions and release of deeper ocean heat than in the Arctic. This strong coupling between the ice and ocean has been invoked as contributing both long-term expansion of the winter ice cover [60], and the dramatic recent retreat [61]. The open northern boundary of the ice pack is exposed to the storms and swell of the Southern Ocean. Here, atmosphere–wave–ice–ocean interactions drive ice production and break-up, ice edge retreat and advance, and a variety of mesoscale phenomena [62]. Along the Antarctic coast, similar processes play important roles in polynyas, where strong winds drive high rates of ice production and export from the coast plays an important role in global water mass transformation. There have been very few direct observations of these processes due to the challenges of operating in these remote and highly dynamic environments (see, e.g., in [63]).

Moorings, ice-tethered platforms, and under-ice profiling floats have provided critical information on these ongoing changes and inter- and intra-seasonal variability, but require significant logistical support to deploy. Moreover, they cannot adequately observe mesoscale phenomena. Larger-scale operations with on-site scientists and technicians are limited by the expense and logistical challenges of operating in this environment. This is particularly true in winter, where large, multidisciplinary expeditions might occur decades apart in some regions (see, e.g., in [63,64]). Under-ice vehicles offer an attractive means to observe ice–ocean interactions in these challenging environments where capturing processes that vary dramatically across small to medium spatial scales are needed, or where traditional methods are exceedingly difficult to perform (see, e.g., in [63,65]). As capabilities advance, particularly for long-term or long-range presence, autonomous under-ice vehicles will play an increasing role in sustained observations of the ice and ocean in both the Arctic and Antarctic [66,67].

### 2.3. Biology

Under-ice ocean worlds belong to the least studied ecosystems on Earth. Therefore, one priority for under-ice robots is the discovery of a highly endemic diversity of life in the Arctic and Antarctic [68]. A key issue is the accessibility of the under-ice life which uses sea ice flows as a substrate, hideout, feeding, and breeding grounds. A number of species are directly connected to life in the ice, including, for example, the colonial sea ice algae *Melosira* which grows into kelp-like forests [11]. ROVs have been used to assess the 3D structure of the under-ice habitat, as well as light transmission, primary productivity, distribution of algae [69], and also the gelatinous life inhabiting the highly stratified water layer under the ice, which is less dense due to the input of ice melt water [70]. Under-ice ROVs or AUVs allow noninvasive studies of the productive layers under the ice and in the upper ice-covered ocean, which can help in quantifying carbon and nutrient budgets, as well as revealing the food webs, diversity, and biological interactions of polar life. Only a few studies have been extended to the deep water and polar ocean seafloor. Early investigations by tethered ROV video surveys of the highly productive Antarctic seafloor assessed composition of benthic communities and the impact of and recovery from iceberg grounding [71]. Modern working class ROVs like *Victor 6000*, *Quest*, and *Kiel 6000* enable experimental studies on factors shaping polar biodiversity (see, e.g., in [72]) in seasonally ice-covered waters, yet they cannot be deployed in full ice. Recent studies of the Arctic ridges, focusing on vents (see, e.g., in [73]) and other prominent habitats associated with the ridges like sponge reefs, cold water corals, and sea mounts, have detected previously unknown, diverse seafloor communities adapted to tap into chemical energy provided from seeping and degassing of hydrogen, sulfur, or hydrocarbons, or from hydrothermalism (see, e.g., in [12,74,75]). Key questions remain as to the effect of climate change, sea ice retreat, glacial melt, and pollution or other forms of human impact on these vulnerable regions of Earth. Some areas that cannot be accessed by ship, like the seafloor under glaciers or thick Antarctic fast ice need first time studies by long range AUVs. ROVs and AUVs have barely been used in polar winter, and key questions remain as to the role and fate of polar life in absolute darkness and coldness of the polar night. The North Pole drift expedition MOSAIC will, for the first time, produce year round under-ice imaging in 3D [76,77]. Accessing polar regions year-round at all depths remains a key task in global ocean observation, management, and protection of ocean life, but needs substantial innovation in reach, navigation, data transmission, and endurance of under-ice robots, especially those equipped with energy-hungry sonars, cameras, and biosensors.

### 2.4. Seafloor Mapping

Seafloor mapping in ice-covered regions offers the same critical geospatial contextual information that it provides in open waters, including the data needed for safe navigation (of both surface and submerged vessels), for defining and understanding benthic habitats, for establishing the routes and dissipation of the deep-sea currents that globally distribute heat, for understanding geologic and tectonic processes (see Section 2.5), for determining the risk of natural hazards (submarine landslides and gas seeps), for revealing a treasure trove of maritime heritage, for predicting tsunami inundation and storm surge run-off, and for exploration and discovery of the 85% of the seafloor that is yet to be mapped. While seafloor and water column mapping from ice breakers is feasible, it is an extremely slow process when done in ice-drift modus, or greatly hampered by the noise generated by ice-breaking. Thus, mapping efforts in ice-covered regions, like those carried out to establish limits of the continental shelf under Article 76 of the United Nations Convention on Law of the Sea [78] are remarkably time-consuming and tend to be conducted as sparsely separated lines rather than the typical overlapping, complete coverage of standard multibeam sonar surveys. The inability to obtain complete overlapping mapping coverage in ice-covered regions greatly reduces the value of these data, as it is often the ability to see the complete picture of the geologic or morphologic context that provides critical insights into seafloor and oceanographic processes.

There are several applications that are particularly critical in ice-covered waters. First among these is the determination of the bathymetry under marine terminating glaciers with ice shelves. Mass loss

from ice sheets in both Greenland and Antarctica has increased dramatically over the past few decades and is a critical contributor to global sea level rise. A key component of the mass loss process, yet one whose quantification is still uncertain, is the contribution from the retreat of marine terminating glaciers forced by oceanic heat transport [79]. The ability of relatively warm waters to interact with marine terminating glaciers is often dependent on the presence or absence of bathymetric sills located under floating ice tongues [33,80], and thus the ability to map under ice-tongues is critical to understanding the fate of terminating glaciers. Additionally, the ability to map the location of grounding lines under ice shelves can provide critical insight into the history and dynamics of the ice sheets [30,31,35,81]. Finally, the history of Arctic glaciation, a fundamental driver of global climate, is recorded on the seafloor (i.e., the recent demonstration that a 1km thick ice sheet covered the central Arctic during the penultimate glaciation [82]) and in the subsurface sediments of the ice-covered regions of the Arctic. Future plans to sample these sediments through scientific drilling will depend on the ability to obtain detailed maps of potential drill sites. Last but not least, high-resolution maps are essential for ecosystem research and as basis for assessing the ecological status of seafloor habitats, and for establishing marine protected areas. New technologies are available to combine mapping and video surveys as an efficient way of creating ecological knowledge of baselines and of disturbances [83,84].

## 2.5. Geology and Geophysics

While ice-tethered profilers have begun to allow routine access to processes at the ice–ocean interface over the past decade or more (see, e.g., in [85]), polar scientists have continued to lack cutting edge capabilities with which to investigate the deep seafloor of both the Arctic and the Antarctic. This has proven particularly frustrating in the context of marine geoscientists interested in the evolution of ocean basins, from three perspectives: (a) in terms of understanding the evolution of the Amerasian Basin in the Arctic, for which numerous, often conflicting, models have been proposed, and (b,c) because the Bransfield Strait in the Antarctic and the Gakkel Ridge in the Arctic represent type localities where geoscientists seek to investigate key processes related to incipient continental rifting and ultra-slow spreading mid ocean ridges, respectively.

For the Amerasian Basin, resolving which of several competing basin evolution models [86–90] is correct remains critical to our understanding of the tectonics of this basin, and therefore its impact on global paleoclimate through the evolution of inter-ocean connections. The paucity of published geophysical data and lack of rock samples from within the basin have made interpretations of the kinematic history of the Amerasia Basin difficult to constrain. The U.S. Extended Continental Shelf Program dredged rock samples from the Chukchi Borderland, Northwind Ridge, and Alpha Ridge using the US Coast Guard Cutter (USCGC) *Healy*. Those samples have brought pre-existing models into question [91], but like all dredged samples, raise the issue of how representative they are of in situ bedrock. Only in situ sampling by a well-positioned underwater vehicle can be guaranteed to provide in situ context and precise location of collected samples.

Studying incipient continental rifting is critical to understanding the evolution of the US Atlantic continental margin. From this perspective, the Bransfield Strait, immediately north and west of the Antarctic Peninsula, rivals the Red Sea (which has even more complex geopolitical barriers to access) as an ideal natural laboratory in which to study such processes—from the first rifting of continental crust through to the opening of ocean basins [92,93]. From shipboard remote-sensing geophysics (seismics, magnetics, and multibeam) data, it is known that the Bransfield Strait rift is comprised of a series of extensional basins that are infilled with detritus from Antarctica. These basins are separated from one another by prominent volcanic constructions that define the rift axis and at least some of which host hydrothermal activity [94–96]. This research has been rather thwarted for more than a decade, however, because no detailed examination of the seafloor geology, including the hydrothermal sites hosted there, have been able to be attempted by ROV.

The Gakkel Ridge, which extends across the entire Arctic Basin from the Norwegian-Greenland Sea to the Siberian Margin represents Earth's slowest spreading and most geologically diverse

mid-ocean ridge, exposing significant outcrops of ultramafic as well as mafic lithologies [15,97] and hosting evidence for geologically recent, and explosive volcanism [12,74,75]. While much has been hypothesized about these processes from remote sensing (including systems mounted on US Navy submarines deployed beneath the ice cap), this ridge system—including the numerous hydrothermal systems that it is known to host [2]—awaits direct intervention by a suitable deep-diving research submersible. This interest has become even more acute in the past decade with the recognition that multiple other planetary bodies in the outer solar system also host saltwater oceans with rocky seafloors beneath their ice shell exteriors [98]. Geothermal systems that can sustain chemosynthetic ecosystems, independent of sunlight, beneath Earth’s ice-covered oceans thus become a compelling analog site for study in the search for life beyond Earth.

## 2.6. Vehicle Capability Needs for Under-Ice Science Missions

The vehicle capability needs for future oceanographic science missions under sea ice and ice shelves naturally depends on the nature of the particular science missions as well as the physical geography of the sea. Although a comprehensive study of vehicle capability needs is beyond the scope of this paper, we note some preliminary observations.

Most ship-based oceanographic operations in the Antarctic occur from November to April. Figure 1 shows, on the left, the Antarctic ice cover in December 2019 and, on the right, the corresponding percentage this ice-covered sea floor for each of 10 depth bins. We note that 40% of the December 2019 ice-covered sea floor has depth between about 3800 m and 5200 m, and that a vehicle with a depth capability of 5200 m could reach 98% of this sea floor. In the Arctic Ocean, the permanently sea ice covered area according to the September sea ice minimum is >1000 m deep, and a vehicle reaching 5000 m would be needed to cover most seafloor area including the North Pole.

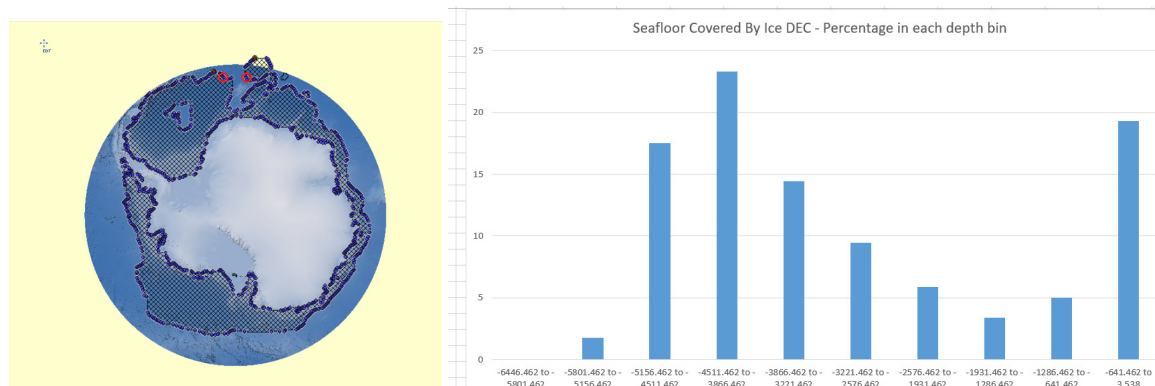


**Figure 1.** Antarctic seafloor covered by ice in December (denoted “DEC” in the figure) 2019 (left figure). Percentage distribution of this ice-covered seafloor in 10 depth bins (right figure).

In terms of horizontal scales, ice shelves can extend from a few kilometers to 1000 km at the most (Filchner–Ronne and Ross), from the calving front to the grounding line. Considering the distance covered by shelf ice, a vehicle with a 400 km range (including the return path) could reach a significant number of targets in a single dive. However, considering the vast area of shelf ice in Antarctica of 1.5 million square kilometers, and that Filchner–Ronne, Ross, and Amery make up most of the area, much longer range capacities are needed for under ice research with at least 1000 km range. Furthermore, a key feature for the future will be the persistent or resident nature of the AUV observations as the need to cover seasonal and interannual variability is extremely important for the coupled ice–ocean interaction physics.

## 3. Under Ice Navigation

Georeferenced navigation is a highly desirable component of modern oceanic science. Georeferenced navigation enables multimodal data sets to be co-registered across multiple dives with

a single asset and across different assets. It enables photographic, bathymetric, and other geophysical maps to be related to generally lower-resolution surface-derived contextual maps. Georeferenced maps yield scientifically relevant context, can reveal features for close inspection and instrument deployment and aid in relocating those features. The Global Positioning System (GPS) does not work underwater, thus alternative navigation methods are required.

For a survey of well-established navigation methods commonly employed for underwater vehicles in temperate latitudes, which is beyond the scope of the present paper, the reader is directed to the work in [99].

Most Uninhabited Underwater Vehicle (UUV) navigation methods beneath permanent moving ice have sought to provide near-ice and ice-relative navigation via acoustic beacons fixed to the ice [100–102] and/or dead-reckoning [103]; however, precedent exists for georeferenced benthic navigation systems as well. The *Theseus* AUV, Figure 2, for example, deployed fiber-optic cable for an under-ice acoustic array utilizing a medium-grade inertial navigation unit and bottom-tracking Doppler Velocity Log (DVL) augmented by a series of widely spaced acoustic beacons placed at critical locations along the vehicle's intended flight path [104]. In 2010–2011, the International Submarine Engineering (ISE) *Explorer* AUV, built for Natural Resources Canada, conducted extensive under-ice seafloor mapping missions in Canada's High Arctic, utilizing a custom 1500 Hz long-range acoustic homing system in addition to a more conventional short-range acoustic homing system [105,106].



**Figure 2.** In 1992, the *Theseus* autonomous underwater vehicle (AUV) laid a fiber-optic cable from Ellesmere Island, Canada, to a remote sea ice camp 175 km from Ellesmere. Image Credit: International Submarine Engineering Ltd. Reproduced with permission.

If communication with the vehicle is available, georeferenced Ultra-Short Baseline (USBL), Two Way Travel Time (TWTT), or One Way Travel Time (OWTT) navigation becomes possible [107]. Both systems rely on being able to telemeter the ship's location to the vehicle. USBL provides a fix directly, whereas OWTT methods require motion on the part of the ship, vehicle, or both. Both systems require the ship to remain within acoustic range of the vehicle and probably could not be used when repositioning the ship to make up for ice drift. On the other hand, neither system requires deploying additional equipment and so the risk of instrument loss is lower than with Long Baseline (LBL) acoustic navigation.

Jakuba et al. reported employing standard oceanographic-grade LBL transponders through the ice to create an otherwise typical deep sea LBL net [108]. Transponders were deployed from

the ship, surveyed by helicopter through open leads of opportunity, and recovered by breaking ice with the ship above their surveyed locations and extracting them from the crush. Deploying beacons on the sea floor always risks the possibility of loss, but that possibility is greatly increased in ice-covered seas. Significant time must also be devoted to transponder survey and recovery. Acoustic beacons therefore represent a proven but time-consuming and potentially costly solution to under-ice navigation. Alternatively, LBL beacons have been deployed fixed to sea ice for operation in a sea ice floe referenced navigation framework [50,51].

Under-ice navigation without the need for LBL transponder deployments has also been investigated. McFarland et al. reported ice-relative navigation utilizing upward-looking DVL, LBL, TWTT and OWTT acoustic ranging, and an Inertial Measurement Unit (IMU) [109].

#### 4. Vehicle Design and Navigation under Ice Shelves and Landfast Sea Ice

Fixed landfast sea ice occurs when sea ice freezes to a shoreline, and may vary in thickness typically up to 10 m. Fixed ice also occurs in the form of ice shelves. An ice shelf is a thick floating slab of ice that forms when a glacier or ice sheet flows into the sea. Ice shelves are typically 100–1000 m thick and can move at a rate of up to several meters per day. Ice shelves are found both in the Arctic and Antarctic. Ice shelves cover 44% of the Antarctic coastline, and can be enormous in area—the largest of which, the Ross Ice Shelf, covers 472,960 km<sup>2</sup>. Retreat and collapse of ice shelves have been extensively documented worldwide [1]. Even strong icebreakers often have no access to such areas, so that the vehicles must be equipped to cover long distances and find their way back. This mostly requires untethered vehicles, but significant work has also been realized by tethered vehicles.

This section reviews previously reported underwater vehicles and navigation systems for use under fixed ice including untethered AUVs, tethered ROVs, and HROVs that can operate with or without a tether.

##### 4.1. Untethered Vehicles

Perhaps the earliest purpose-built under-ice vehicle was the *Unmanned Arctic Research Submersible System* (UARS), first deployed in 1972. Communication and navigation with the 450 m depth capable vehicle was achieved with a 50 kHz LBL acoustic positioning and communication system, which consisted of four free-floating transducers which were typically deployed through the sea ice near the deployment area. Vehicle recovery was performed by lowering a net outfitted with a homing beacon into the hole through which UARS was deployed. Once within range of the homing beacon UARS would navigate towards the beacon, and become ensnared in the net by means of barbed hook mounted on the nose cone of the vehicle [110].

The *Autonomous Remotely Controlled Submersible* (ARCS) was developed by ISE to conduct bathymetric surveys in the Arctic. The vehicle was equipped with a DVL, gyrocompass, LBL positioning system, and obstacle avoidance sonars, and was first operated in an untethered manner in 1982 [111–113].

Light and Morison [114] describe the design and 1989 deployments of the *Autonomous Conductivity Temperature Vehicle* (ACTV). Derived from a US Navy Mark-38 sonar target, the ACTV was outfitted with three-axis (non-gimbaled) magnetometer, depth, and pitch/roll sensors. Modified to accommodate a SeaBird CTD sensor, the vehicle was programmed to conduct transects at predetermined depth and heading combinations before navigating to the recovery site using an acoustic homing beacon.

Nicholls et al. describe the *Autosub2* AUV and the 2005 under-ice missions conducted at the Fimbul Ice Shelf, Antarctica [115]. *Autosub2* was a long-range vehicle (400 km) and was outfitted with a Fiber-optic Gyroscope (FOG) gyrocompass and upward- and downward-looking DVL to provide dead reckoning capability. Deployed on 13 February 2005, *Autosub2* navigated approximately 26 km beneath the Fimbul Ice Shelf, collecting upward-looking ice topography and physical oceanographic data. While *Autosub2* failed to return from beneath Fimbul on the subsequent mission, the body of scientific work that resulted from the vehicle's 383 missions is substantial. Prior to the Fimbul Ice Shelf

missions, *Autosub2* mapped landfast sea ice over 450 km of mission-track on the Greenland coast in 2004 [49].

Following the loss of *Autosub2*, *Autosub3*, Figure 3, was developed with increased attention to robustness and redundancy of critical systems, and was successfully deployed beneath the Pine Island Glacier (PIG), Antarctica in January 2009 [30,32,116] and 2014 [36,41]. A navigation sensor suite similar to that of *Autosub2* allowed the vehicle to navigate a total of 511 km beneath PIG over the course of six missions in 2009 and four missions in 2014. Sonar and physical oceanographic data collected during those missions shed light on the rapid ice shelf thinning and retreat of the PIG grounding line.

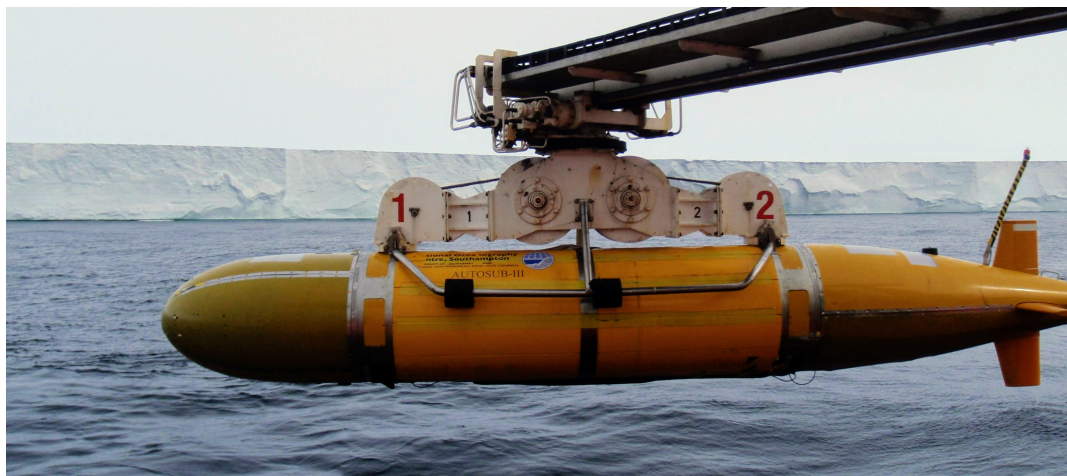


**Figure 3.** AUV *Autosub 3* aboard the R/V *Nathaniel B. Palmer* after successful missions under Pine Island Glacier (background), Amundsen Sea, Western Antarctica, in 2009. Image Credit: Pierre Dutrieux.

Most recently, the Autosub Long Range AUV *Boaty McBoatface* was deployed in 2018 beneath the Filchner and Ronne ice shelves in Antarctica to make direct measurements of ice shelf and seabed morphology, and to investigate controlling factors for the flow of melt waters. A magnetic compass combined with upward- and downward-looking DVL were used to produce a Dead Reckoning (DR) navigation solution [117].

Forrest et al. report on the 2007 deployments of the *UBC-Gavia* AUV in the freshwater Pavilion Lake, British Columbia, Canada. The *UBC-Gavia* is navigated either by inertial DR or acoustic LBL. A commercially available 457 kHz avalanche beacon was used to aid in recovery should the vehicle not return to the deployment hole. Tests reported in [118] showed that when the vehicle was directly beneath the ice, the beacon signal could be received from atop the ice at horizontal ranges up to 40 m, and used to localize the vehicle beneath the ice to an accuracy of 5–8 m. *UBC-Gavia* has also been deployed in multiple ocean settings, both in the Arctic and Antarctic, though a light tether was attached to ensure vehicle recovery [119–121].

In December 2008, the *ENDURANCE* AUV was deployed through a melt hole into Lake Bonney, Taylor Valley, Antarctica to conduct three-dimensional chemical and spatial mapping [122]. *ENDURANCE*'s principal navigation system consisted of a DVL-aided Inertial Navigation System (INS) and USBL system. The authors describe a custom magnetic beacon system which, when used in conjunction with a Real-Time Kinematic GPS, was used to provide cm-level localization when *ENDURANCE* was located directly beneath the ice. The robot used a machine vision-based system for returning to the deployment hole. Additional information on *ENDURANCE*'s navigation system can be found in [123].

Kukulya et al. report on the March 2010 Arctic deployments of a *Remote Environmental Monitoring UnitS* (REMUS) 100 AUV to collect oceanographic data near Barrow Alaska [124]. A combination of LBL, USBL, and OWTT acoustic systems complemented the compass and DVL-based DR system already implemented on the REMUS. Following several tethered test runs, the vehicle completed four untethered survey missions, each ending with net capture and recovery similar to that described in [110].

Hildebrandt et al. of the German Research Center for Artificial Intelligence reported in 2013 on the design of an under-ice AUV in support of the European Europa-Explorer project [125]. The vehicle will be equipped with an acoustic navigation suite to allow LBL, USBL, and OWTT navigation. Hildebrandt et al. also report the vehicle will contain upward- and downward-looking DVLs and a FOG for inertial DR.

Forrest et al. report on the 2014 deployments of a Teledyne *Gavia*-class AUV in McMurdo Sound, Antarctica. The vehicle was outfitted with a multispectral radiometer and was deployed through annual sea ice to conduct irradiance measurements, with the goal of better characterizing the spatial heterogeneity of sea ice algae [126].

In 2018, the AUV *nupiri muka*, a 5000 m rated ISE Explorer operated by the University of Tasmania, Australia, was deployed beneath the Sørsdal Glacier near Davis Research Station, Antarctica. Three initial dives were conducted over eight days and included transits up to 700 m beneath the floating glacier [127].

A similar feat was achieved in 2019 by a Hugin AUV operated by the University of Gothenburg, Sweden, which was deployed for a few kilometers beneath the floating tongue of Thwaites Glacier in West Antarctica [128].

In February of 2020, engineers from Monterey Bay Aquarium Research Institute (MBARI) and Woods Hole Oceanographic Institution (WHOI) deployed a *Tethys*-class AUV beneath lake ice in northern Maine, United States. Deployments were conducted in conjunction with the United States Coast Guard, and the efforts aim to allow mapping and investigation of underwater oil spills in ice-covered waters. A through-ice acoustic/RF gateway buoy was used to provide position corrections, communications, and docking capabilities to the vehicle, which uses a DVL and Micro-electro-mechanical systems (MEMS)-based IMU dead reckoning for navigation [129].

#### 4.2. Tethered Vehicles

Tethered vehicles are difficult to operate under ice shelves and landfast sea ice because the tether must either be deployed from a vessel or ice camp at the seaward ice-edge, or a hole must be drilled through the ice to provide a passage to deploy the vehicle and tether directly through the ice. Moreover, conventionally tethered ROVs typically provide very limited horizontal excursion from the ship or ice-camp from which they are deployed.

The *ROBY* ROV, as described by Bono et al. and Veruggio et al. [130,131], was developed by the Italian National Research Council and underwent engineering trials in Terra Nova Bay, Antarctica in austral summer 1993/94. *ROBY* was equipped with inclinometers, a magnetic compass, and angular and linear accelerometers, and tests on closed-loop heading and depth control are presented in [131].

The National Aeronautics and Space Administration (NASA) *Telepresence-Controlled Remotely Operated Vehicle* (TROV) consists of a modified *Phantom S2* ROV and was deployed in the McMurdo Sound, Antarctica in 1993 [132]. The vehicle was navigated using a SHARPS Short Baseline (SBL) system consisting of three transducers deployed through sea ice, arranged in an equilateral triangle (100 m legs) above the workspace of interest, with two transducers mounted on the vehicle. Of note is that telepresence operation of the vehicle from NASA Ames Research Center, in Mountain View, CA, USA, was achieved via off-continent satellite connection.

Caccia et al. [133] report on the design and testing of the *ROMEO* ROV in Terra Nova Bay, Antarctica during the austral summer 1997/98. Configured with a DVL, gyroscope, compass, and inclinometers, Caccia et al. present results from sea floor and ice canopy following transects.

In 2008, Vogel et al. described the *Sub-Ice ROV* (SIR) for deployments beneath Antarctic ice sheets. Designed and built by DOER Marine, SIR is intended for deployment through surface-melted boreholes, and is outfitted with FOG and dual DVLs that enable DR navigation [134].

The *Submersible Capable of under Ice Navigation and Imaging* (SCINI) ROV (Figure 4), developed at Moss Landing Marine Laboratories, is designed to allow exploration and research of the under-ice seafloor. Departing from the traditional model of ship-based underwater vehicles, SCINI is deployed

through holes drilled through a range of Antarctic ice, and notably can fit (with operations team and ancillary equipment) in a single helicopter [135]. SCINI has utilized LBL, SBL, and most recently a USBL navigation system [136] during a 2012–2015 field campaign surveying biomass at distinct trophic levels in the McMurdo Sound.



**Figure 4.** The ROV Submersible Capable of under Ice Navigation and Imaging (SCINI) and Fluorometer and Acoustic Transducer Towable Instrument (FATTI) being deployed through landfast sea ice to map spatial and temporal distributions of chlorophyll (phytoplankton proxy), crystal krill—*Euphausia crystallorophias*, and Antarctic silverfish—*Pleuragramma antarcticum* in the McMurdo Sound, Antarctica in November 2014. Image Credit: S. Kim. Reproduced with permission.

Behar et al. [137] discuss the design, testing, and deployments of the *Micro Subglacial Exploration Device* (MSLED) ROV. Weighing just under 2.9 kg, MSLED was designed to provide visual survey and horizontal CTD measurement capability in Subglacial Lake Whillans (SLW), Antarctica. Heading and attitude estimation are provided by a MEMS IMU. MSLED was successfully tested in the McMurdo Sound during austral summer 2012/13, but due to complications that arose in the field, the vehicle was not deployed into SLW.

A system-level design and description of Antarctic deployment of *Deep-SCINI* is presented by Burnett et al. in [138]. Deployed through a 740 m borehole during the austral summer 2014/15, *Deep-SCINI* provided visual inspection capabilities and CTD measurements near the grounding zone of the Ross Ice Shelf. Of scientific note was the discovery of macrofauna near the ice shelf's grounding line, over 800 km from open ocean.

Spears et al. report on the development of *Icefin*, a borehole-deployable vehicle [139]. As initial fielding of a prototype in 2014, the redeveloped *Icefin* vehicle [140] has conducted three austral summer field seasons (2017 through 2020) deploying through the sea ice adjacent to McMurdo station, as well as surveying under the front of the McMurdo Ice Shelf and mapping the grounding zone of Erebus Glacier tongue, amassing over 160 h under ice and tens of kilometers of surveys.

During the Austral summer of 2019/20, two Icefin vehicles were deployed at two different sites through 600 m thick ice via hot water drilled boreholes. As part of the NERC-NSF International Thwaites Glacier Collaboration, Icefin aims to improve understanding of contributions to sea level rise by Thwaites Glacier by providing the first three-dimensional surveys of the grounding zone of a major glacier system, which were completed in January 2020. A KVH 1775 IMU, Navquest NQ600 micro DVL, and Valport ultraP pressure sensor provide measurements to an Extended Kalman Filter (EKF) to compute onboard navigation estimates [141].

Klesh et al. report the development and polar field evaluation of a *Buoyant Rover for Under-Ice Exploration* (BRUIE), a prototype of future rovers to explore ice covered oceans such as that of Jupiter's moon Europa, which uses actuated wheels and positive buoyancy to traverse along the underside of ice [142,143].

#### 4.3. Hybrid Tethered Vehicles

Hybrid tethered vehicles (also referred to as "lightly tethered vehicles") represent a relatively new class of vehicle in which the vehicle's tether only provides a telemetry link (electrical or optical), but does not provide electrical power to the vehicle. Such tethers typically do not act as a strength member, and may be expendable, and thus cannot be relied upon to aid in vehicle recovery. Lightweight hybrid fiber-optic tethers are proving to be robust in under-ice operations, provide very high bandwidth telemetry for data and imaging, and support very large horizontal and vertical vehicle excursions from the deployment location. These vehicles have on-board power storage, typically Lithium-Ion battery packs. Vehicles employing expendable tethers typically are equipped with underwater acoustic modems to provide bidirectional command and data telemetry in the event of tether failure.

During the austral summer 2015/16, *ARTEMIS*, a modified and low-drag variant of the *ENDURANCE* vehicle, was deployed beneath the Ross Ice Shelf, Antarctica. Clark reports under-ice navigational accuracy of 0.1% distance traveled during a 5 km transect [144].

### 5. Vehicle Design and Navigation under Moving Sea Ice

Sea ice is formed when the ocean surface freezes. Moving sea ice is found extensively both in the Arctic and Antarctic, and constitutes most of the sea ice in the Arctic and Antarctic year-round, but with large seasonal and interannual variability. Moving pack ice presents unique challenges to underwater vehicle deployment and navigation that are not present for immobile fast ice or ice shelves. This section reviews previously reported underwater vehicles and navigation systems for use beneath moving ice including untethered AUVs and gliders, tethered ROVs, and HROVs that can operate with or without a tether.

#### 5.1. Untethered Vehicles

In 1992, ISE and the Canadian Department of National Defence began development of the *Theseus* AUV, Figure 2. Ferguson et al. [145] present an overview of *Theseus*'s motivation, subsystems, trials, and primary mission: laying a fiber-optic cable from the coast of Ellesmere Island, Canada, to a remote sea ice camp 175 km from Ellesmere. As deployed, *Theseus* was equipped with a Ring-laser Gyroscope (RLG) gyrocompass, DVL, LBL positioning system, and homing beacon. To bound *Theseus*'s DR error, six LBL acoustic transducers were deployed along the AUV's intended path—through sea ice—prior to mission commencement. *Theseus* successfully completed its cable laying mission and returned to the deployment location, traveling over 350 km beneath ice. Additional (and more technical) details on *Theseus* can be found in [146].

An *Odyssey II*-class vehicle was configured for Arctic operations and is described by Bellingham et al. [147]. The vehicle was configured with a magnetometer, six-axis IMU, depth, LBL, and USBL acoustic packages. Bellingham et al. present results from several methods of vehicle navigation employed in *Odyssey*'s 1993 deployments, including DR, vehicle-mounted USBL, and USBL-corrected Kalman filtered DR.

Hayes and Morison [148] describe the *Autonomous Microconductivity Temperature Vehicle* (AMTV). Based upon the REMUS vehicles developed at WHOI, and equipped with a Sytron Donner Motion Pack, LBL, and homing beacon acoustic packages, AMTV was deployed during the SHEBA experiment in 1998 to measure salt and heat fluxes beneath melting sea ice in the Arctic. The LBL network was comprised of hydrophones lowered to 15 m depth, in 50–100 m spacing around the survey sites. Over the course of the 27 day experiment, AMTV conducted 70 km of survey tracks, while the ice floe drifted approximately 180 km.

Wadhams et al. report the commercially available *Martin 150* AUV was deployed in the Arctic in 2002 to measure ice draft in the Marginal Ice Zone (MIZ) [149]. They report a navigation system consisting of a RLG, DVL, and Differential GPS (for use at the surface). Equipped with side-scan sonar, two missions were undertaken to measure ice draft, with the vehicle traveling 3.6 km in total.

McEwen et al. [103] discuss the selection and 2001 Arctic trials of several navigation systems for the MBARI ALTEX AUV. Results are presented on several tests, including navigation sensor alignment, performance of DVL ice-tracking, comparison of magnetic and gyrocompass heading error, and overall vehicle navigation error.

Brierly et al. report observations of Krill up to 27 km under the Antarctic sea ice edge with *Autosub2* in 2001, the first AUV missions under Antarctic pack ice [150].

In summer of 2007, two Seabed-class AUVs—*Jaguar* and *Puma*—were deployed at sites along the Gakkel Ridge near 85°N 85°E [151]. Scientific missions conducted with the vehicles consisted of chemical, physical, and oceanographic surveys, with the vehicles utilizing a combination of DVL-corrected inertial navigation and seafloor-suspended LBL network for navigation [108]. LBL beacons were also suspended from the ship to aid vehicle recovery by providing ship-relative navigation.

Using data collected in 2008, Kimball and Rock present proof-of-concept results in [152] for a Terrain Relative Navigation (TRN) algorithm capable of localizing an underwater vehicle relative to a free-floating iceberg. Their two-step approach is comprised of an initial mapping run, followed by deployments in which the vehicle can localize itself relative to the iceberg. Their algorithm estimates and accounts for iceberg rotation and translation in the vehicle's position estimation.

Jalving et al. report on the upgrades and 2008 trials of a Kongsberg *HUGIN 1000* AUV for under ice operations. In addition to the DVL and USBL/LBL-aided INS, an RF-based under-ice localization and communication system was demonstrated, and is capable of communication with *HUGIN* while 60 m beneath sea ice by means of a remotely controlled model helicopter [153].

Following the success of the *Theseus* AUV, two ISE *Explorer* AUVs, Figure 5, were built and deployed in 2010 in the Canadian Arctic to conduct bathymetric surveys to support Canada's claim to the extent of its continental shelf under the United Nations Law of the Sea Convention. *Explorer's* extensive navigation system, described in [106,154], consists of a DVL-aided INS, USBL, and a custom short-range localization system and homing system. Of technical note is the development of custom 1376 Hz homing system reported in [106]. Crees et al. note that the homing system was instrumental to *Explorer's* successful navigation. Drifting of the remote ice camp, and DR error accumulation meant that *Explorer's* recovery location could be >30 km away from the expected location. The custom homing solution proved successful at ranges of 50 km, and is expected to function at ranges >100 km. In total, *Explorer* logged near 1000 km over three missions, at depths up to 3160 m.

In 2007, the first digital terrain mapping of the underside of drifting pack ice was done over a small area with a *Gavia* AUV [155]. Although operating autonomously, the vehicle was tethered to aid recovery.

In 2010 and 2012, WHOI Seabed-class AUVs (Figure 6) were deployed in the Weddell and Bellingshausen Seas and East Antarctic waters to conduct high-resolution ice draft measurements. Williams et al. report in [50] that the vehicles utilized an ice-relative navigation system, consisting of LBL beacons deployed beneath sea ice outside of the intended work volume, and the vehicles were outfitted with an upward-looking DVL and FOG gyrocompass. Similar work was also performed

in the autumn Arctic marginal ice zone in 2015 [65], and in the winter Ross Sea ice pack in 2017 [51]. For these campaigns, maintaining an accurate ice-references navigation frame was critical so that the under ice observations could be precisely co-located with above ice mapping.



**Figure 5.** Two ISE *Arctic Explorer* AUV aboard ISE's R/V *Researcher* Nanoose Bay, BC, Canada during sea trials in 2010. The ISE *Arctic Explorer* AUV were built and deployed in the Canadian Arctic to conduct bathymetric surveys to support Canada's claim to the extent of its continental shelf under the United Nations Law of the Sea Convention. Image Credit: International Submarine Engineering Ltd. (Port Coquitlam, BC, Canada) Reproduced with permission.

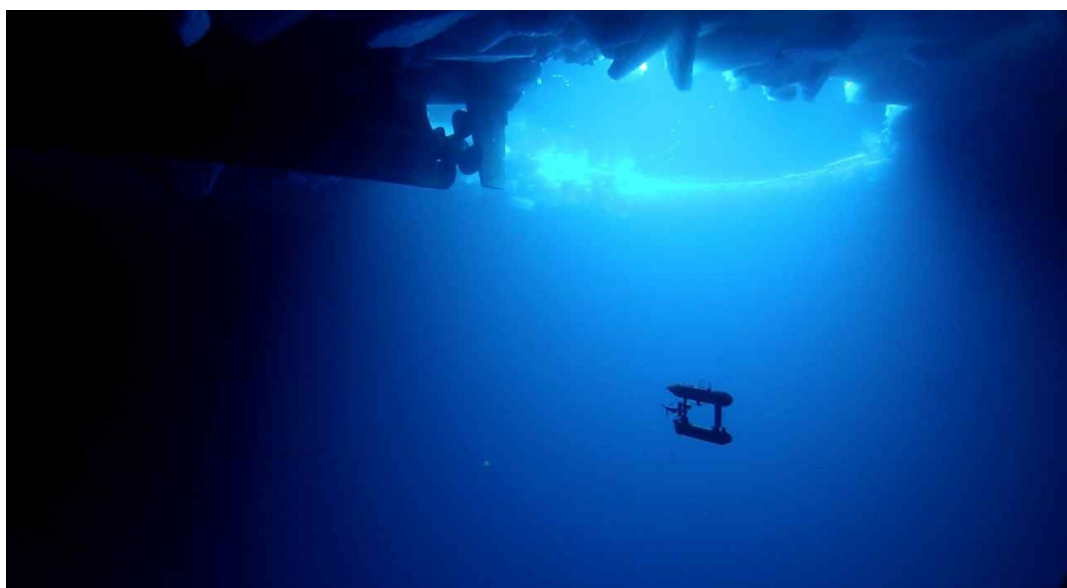


**Figure 6.** The Seabed-Class *Jaguar* AUV conducting an upward-looking multibeam survey of Antarctic sea ice with the R/V *Aurora Australis* visible in the background. Image Credit: K. Meiners, G. Williams, and H. Singh, Australian Antarctic Division and Woods Hole Oceanographic Institution. Reproduced with permission.

Wulff et al. reported on the 2013 deployments of the *Polar Autonomous Underwater Laboratory* (PAUL), a *Bluefin 21* AUV, in Fram Strait, Figure 7. The vehicle was outfitted with a suite of physical and biogeochemical oceanographic sensors [156,157], and was tasked with collecting data in the meltwater front of the MIZ. Because the vehicle was operating in mid-water, navigation aiding was provided by a ship-mounted iXBlue GAPS USBL [8,9,158].



**Figure 7.** The *Polar Autonomous Underwater Laboratory* (PAUL), a *Bluefin 21* AUV, equipped with physical and biogeochemical oceanographic sensors and a water sampler, observed biogeochemical processes at high resolution in the marginal ice zone of Fram Strait. Image Credit: Alfred Wegener Institute, Helmholtz Centre for Polar and Marine Research. Reproduced with Permission.

In July of 2017, the iceberg mapping work was conducted near Sermilik Greenland, with the deployment of MBARI's. *Dorado* class AUV. The vehicle is outfitted with precision RLG, and DVL, and two Imagenex 220 kHz DeltaT 837A multibeam sonars were used for mapping and obstacle avoidance. An iceberg of 200 m draft and 1200 m in waterline width was autonomously mapped and encircled over the course of 13 missions at depths of 50, 100, and 150 m [159].

### 5.2. Tethered Vehicles

Tethered underwater vehicles are challenging to deploy from ships in sea ice because the ice floes can damage and/or cut the tethers, the ships typically cannot maneuver while tethers are deployed over the side, and conventionally tethered ROVs typically provide very limited horizontal excursion from the ship from which they are deployed.

In 2002 and 2005, the ROV *Global Explorer* was deployed in the Arctic Ocean from the USCGC *Healy* during the NOAA Hidden Ocean Expedition [68,160]. *Global Explorer* was used to conduct visual surveys and specimen collection of gelatinous taxa.

A modified *Phantom S2* ROV (Deep Ocean Engineering, San Jose, CA, USA) was used by Hobson et al. during expeditions aboard the R/V *N.B. Palmer* in 2005, 2008, and 2009 to survey the underwater environments surrounding free-floating icebergs near Antarctica [161]. Battery-powered beacons on the ROV provided pilots with ROV-ship range measurements, while a scanning sonar mounted on the Phantom was used to navigate alongside and maintain desired standoff distance from the iceberg.

Nicolaus and Katlein [162] report on Arctic deployments of a V8ii ROV (Ocean Modules, Åtvidaberg, Sweden) from the F/S *Polarstern* in 2011. The vehicle was outfitted with spectral radiometers, and combined with a 300 m tether, was tasked with mapping under-ice spectral radiance and irradiance. Scientific results include optical surveys of ice algae chlorophyll concentrations [163], and studies of light transmission through the Antarctic pack ice [164]. More recently they report the development and deployment of a new ROV based upon the *Ocean Modules M500* ROV (Ocean

Modules, Sweden) as a highly instrumented sensor platform for interdisciplinary research at the ice–water interface [69].

In 2013, Arndt et al. performed ROV transects beneath sea ice in the northern Weddell Sea, Antarctica to examine the influence of snow depth and flooding on light transmission through Antarctic sea ice. A network of 4 Benthos XT-6001 transponders were placed in a 400 m-side rectangle, with co-located GPS, to provide a through-ice LBL network for localization [164].

### 5.3. Hybrid Tethered Vehicles

The *Nereid Under-Ice* (NUI) vehicle, Figure 8, is a lightly-tethered hybrid AUV/ROV (HROV) developed by WHOI and collaborators at Johns Hopkins University [165]. Designed to be operated under fixed or moving ice, NUI is capable of standoff distances up to 20 km from the deployment vessel, and is equipped with a navigation suite including LBL and OWTT acoustic packages, a FOG IMU, and upward- and downward-looking DVLs [109]. McFarland et al. describe the ice-relative navigation algorithm as implemented during July 2014 operations at 83°N 6°W from icebreaker F/S *Polarstern*. Katlein et al. present under-ice light transmission data from some of NUI’s first science operations at the ice–ocean interface, in July 2014 [166]. Figure 9 shows example of high resolution multibeam bathymetry of the Karasik Seamount collected during NUI’s first under-ice seafloor surveys in 2016 at 87°N 61°E.

Zeng et al. report on the 2014 deployment of *Polar-ARV* during the sixth Chinese National Arctic Research Expedition (CHINARE) [167]. *Polar-ARV* is a lightly tethered vehicle with a 100 m depth rating, 3 km operating radius, and was deployed via a hole drilled through sea ice adjacent the Icebreaker *Snow Dragon*.



**Figure 8.** Hybrid ROV/AUV *Nereid Under-Ice* (NUI) deployment from the F/S *Polarstern* in July 2014 at 83°N 6°W in July 2014. The mated tow-body (orange) and depressor (white) suspended above the vehicle house NUI’s unarmored fiber-optic telemetry system. Actuation of an electromechanical latch separates the tow-body from the depressor at a suitable depth, after which fiber pays out of either body to accommodate the relative motion of the vehicle and ship. Image Credit: L. L. Whitcomb.

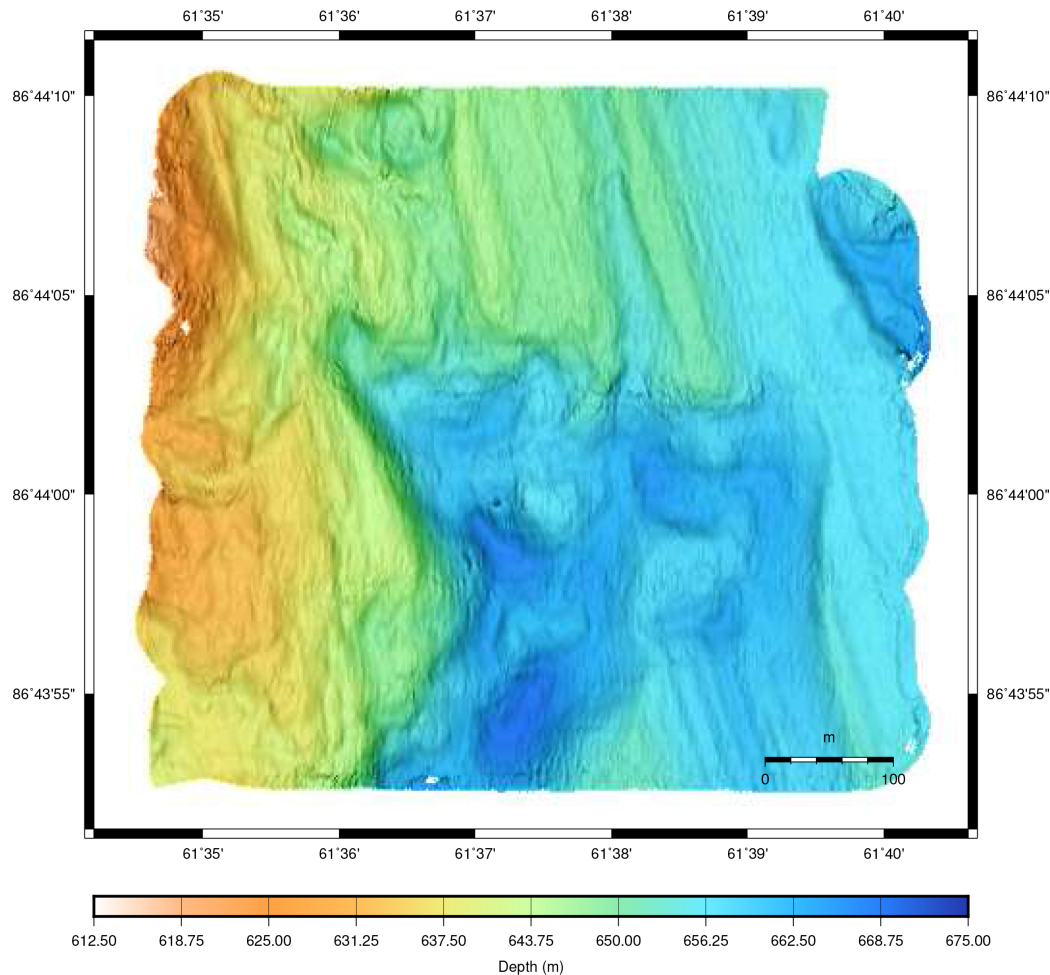


**Figure 9.** High-resolution multibeam bathymetry of an area  $600\text{ m} \times 550\text{ m}$  mapped using the *Nereid Under-Ice* (NUI) hybrid vehicle in AUV mode at the Karasik Seamount at  $87^\circ\text{N}$   $61^\circ\text{E}$ , beneath 100% ice-cover, in a September 2016 deployment from the F/S *Polarstern*.

#### 5.4. Underwater Gliders

Gliders are a unique class of underwater vehicle that do not rely upon traditional propeller propulsion for forward motion. They were first proposed in the 1960s, but were not demonstrated as a viable AUV concept until the early 2000s [168]. To achieve forward propulsion, gliders typically combine a buoyancy engine, adjustable center of mass, and horizontal wings to propel the vehicle in a sawtooth pattern through the water. Gliders are energetically efficient vehicles, but are limited in their forward velocity compared to traditionally propelled vehicles. Recent studies have examined the feasibility of hybrid underwater glider designs that combine buoyancy-driven glider propulsion with conventional propeller propulsion [169]. For a comprehensive review of glider history, development, and governing principles, readers are directed to the work in [168].

Jones et al. [170] report on the deployment of eight *Slocum* Gliders in the waters around Antarctica during the austral summer of 2010/11. Outfitted with various physical and biological oceanography instruments, the vehicles mapped spatial extent of distinct water masses and their features to inform concurrent ship-based sampling.

In [171], Zhou et al. report on the integration of a mechanical scanning sonar (Tritech Micron) into a *Slocum* Glider for the purposes of iceberg survey and mapping off the coast of Newfoundland, Canada. A detailed discussion of the iceberg search and acoustic processing algorithms is given, along with results of the in situ and postprocessed volume estimates for the target icebergs encountered during field trials.

The University of Washington's Applied Physics Laboratory has been deploying *Seaglider* AUVs in Davis Strait for over a decade [172]. In 2014, a multi-month deployment of *Seaglider* AUV (Figure 10) was conducted to monitor the seasonal melt of the MIZ near 72°N 145°W [173]. Webster et al. describe an array of through-ice buoys, as well as autonomous surface craft outfitted with acoustic hardware to provide the gliders a means of localization. A OWTT navigation algorithm was implemented on the vehicles, with buoys broadcasting time-of-launch-encoded position packets at regularly timed intervals. Reliable beacon–glider ranges were achievable at distances of up to 400 km, even when the vehicles were not in the strong sound duct present at 100 m depth. As far as the authors could discern from published works, this deployment represents the longest term under-ice deployment of AUVs to date.



**Figure 10.** The University of Washington's Applied Physics Laboratory has deployed Seagliders extensively under sea ice of the MIZ near 72°N 145°W. Image Credit: Applied Physics Laboratory, University of Washington. Reproduced with permission.

The University of Washington Applied Physics Laboratory has continued its under ice glider work, and in late 2016 began the Stratified Ocean Dynamics of the Arctic (SODA) experiment, a multi-year coordinated experiment with twelve other institutions. *Seaglider* AUVs are being employed to measure temperature, salinity, dissolved oxygen, and downwelling irradiance during one year deployments in ice covered waters. Navigation capability is provided by on-board dead reckoning, with position corrections provided by permanently moored acoustic beacons [66].

Building on proven under sea ice capabilities, UW-APL collaborated with Lamont–Doherty Earth Observatory to realize *Seaglider* deployments beneath the Dotson Ice Shelf, Antarctica, between January 2018 and January 2019. The vehicles made a total of 18 trips beneath the ice shelf, with the longest excursion being 140 km beneath the shelf [174].

## 6. Conclusions

The 12% of the world's oceans that is covered by fixed or moving ice remains largely inaccessible to ocean science. Over the last three decades, researchers have developed and deployed multiple new classes of underwater robotic vehicles and navigation methods specifically to provide scientific access beneath ice shelves, landfast ice, and free-floating ice. However, fundamental obstacles remain that severely limit under-ice oceanographic vehicle operations in ice-covered environments including vehicle launch, recovery, and navigation. Successful ship-based under-ice operations are subject to favorable weather and ice conditions, whereas landfast and through-ice vehicle deployments require specialized ice drilling or melting equipment, which also significantly constrain vehicle size,

shape and endurance. Navigation beneath both moving and stationary ice remains challenging, both at depth and near the surface.

Nearly two decades ago, Edmonds et al. [2] discovered abundant hydrothermal venting along the 1100 km Gakkel Ridge in the Arctic Ocean, clearly indicating the existence of 9–12 discrete active hydrothermal vent sites, but specific active vent sites on the Gakkel Ridge have yet to be explored. Similarly, exploration of ice shelf cavities only started a decade ago, and only half a dozen cavities have been partially or comprehensively observed to date, in general for a limited amount of time (hours to days). Under sea ice, passive drifting platforms and manned icebreakers and ice stations have been used for decades, but observations remain sparse compared to the open ocean, particularly in winter. UUVs have only just begun to be routinely exploited, with most covering only limited ranges and/or durations, and with efforts for sustained observations or long-range missions only just emerging. The potential for first-order scientific discoveries at high latitudes, under ice, remains high, but new and improved approaches to the design and navigation of underwater vehicles will be needed to achieve this.

**Author Contributions:** Conceptualization, L.D.L.B. and L.L.W; writing—original draft preparation, all Authors; writing—review and editing, all Authors. All authors have read and agreed to the published version of the manuscript.

**Funding:** Barker and Whitcomb gratefully acknowledge the support of the National Science Foundation under Award 1319667 and 1909182, and support of the first author under a Graduate Fellowship from the Johns Hopkins Department of Mechanical Engineering. Jakuba, Bowen, and German gratefully acknowledge the support of the National Aeronautics and Space Administration under Planetary Science and Technology through Analog Research (PSTAR) award NNX16AL04G. Maksym was supported by National Science Foundation Award CMMI-1839063. Dutrieux was supported by his Center for Climate and Life Fellowship from the Earth Institute of Columbia University. Boetius acknowledges funding from the Helmholtz Association for the FRAM infrastructure, and from her ERC Adv. Grant ABYSS (294757). Mayer’s work is supported by NOAA Grant NA15NOS4000200.

**Conflicts of Interest:** The authors declare no conflicts of interest. The funders had no role in the design of the study; in the collection, analyses, or interpretation of data; in the writing of the manuscript; or in the decision to publish the results.

## Abbreviations

The following abbreviations are used in this manuscript.

ACTV	<i>Autonomous Conductivity Temperature Vehicle</i>
AMTV	<i>Autonomous Microconductivity Temperature Vehicle</i>
ARCS	<i>Autonomous Remotely Controlled Submersible</i>
AUV	<i>Autonomous Underwater Vehicle</i>
BRUIE	<i>Buoyant Rover for Under-Ice Exploration</i>
CTD	<i>Conductivity Temperature Depth</i>
DR	<i>Dead Reckoning</i>
DVL	<i>Doppler Velocity Log</i>
EKF	<i>Extended Kalman Filter</i>
FATTI	<i>Fluorometer and Acoustic Transducer Towable Instrument</i>
FOG	<i>Fiber-optic Gyroscope</i>
GPS	<i>Global Positioning System</i>
HOV	<i>Human Occupied Vehicle</i>
HROV	<i>Hybrid Remotely Operated Vehicle</i>
IMU	<i>Inertial Measurement Unit</i>
INS	<i>Inertial Navigation System</i>
ISE	<i>International Submarine Engineering</i>
LBL	<i>Long Baseline</i>
MBARI	<i>Monterey Bay Aquarium Research Institute</i>
MEMS	<i>Micro-electro-mechanical system</i>

MIZ	Marginal Ice Zone
MSLED	<i>Micro Subglacial Exploration Device</i>
NUI	<i>Nereid Under-Ice</i>
OWTT	One Way Travel Time
PAUL	<i>Polar Autonomous Underwater Laboratory</i>
PIG	Pine Island Glacier
REMUS	<i>Remote Environmental Monitoring Units</i>
RF	Radio Frequency
RIS	Ross Ice Shelf
RLG	Ring-laser Gyroscope
ROV	Remotely Operated Vehicle
SBL	Short Baseline
SCINI	<i>Submersible Capable of under Ice Navigation and Imaging</i>
SIR	<i>Sub-Ice ROV</i>
SLAM	Simultaneous Localization and Mapping
SLW	Subglacial Lake Whillans
SODA	Stratified Ocean Dynamics of the Arctic
TRN	Terrain Relative Navigation
TROV	<i>Telepresence-Controlled Remotely Operated Vehicle</i>
TWTT	Two Way Travel Time
UARS	<i>Unmanned Arctic Research Submersible System</i>
USBL	Ultra-Short Baseline
UUV	Uninhabited Underwater Vehicle
WHOI	Woods Hole Oceanographic Institution
MOR	Mid-Ocean Ridge

## References

- Weeks, W. *On Sea Ice*; University of Alaska Press: Fairbanks, AK, USA, 2010.
- Edmonds, H.N.; Michael, P.J.; Baker, E.T.; Connelly, D.P.; Snow, J.E.; Langmuir, C.H.; Dick, H.J.B.; Mühe, R.; German, C.R.; Graham, D.W. Discovery of abundant hydrothermal venting on the ultra-slow spreading Gakkel Ridge, Arctic Ocean. *Nature* **2003**, *421*, 252–256. [[CrossRef](#)] [[PubMed](#)]
- Smethie, W.M.; Chayes, D.; Perry, R.; Schlosser, P. A lightweight vertical rosette for deployment in ice-covered waters. *Deep. Sea Res. Part I Oceanogr. Res. Pap.* **2011**, *58*, 460–467. [[CrossRef](#)]
- Nansen, F. *Farthest North: Being the Record of a Voyage of Exploration of the Ship "Fram" 1893–1896 and of a Fifteen Months' Sleigh Journey by Dr. Nansen and Lieut. Johansen (Complete)*; Macmillan and Company: London, UK, 1904; Volume 1.
- Bourke, R.H.; Garrett, R.P. Sea ice thickness distribution in the Arctic Ocean. *Cold Reg. Sci. Technol.* **1987**, *13*, 259–280. [[CrossRef](#)]
- Jakobsson, M.; Grantz, A.; Kristoffersen, Y.; Macnab, R. Physiographic provinces of the Arctic Ocean seafloor. *Geol. Soc. Am. Bull.* **2003**, *115*, 1443–1455. [[CrossRef](#)]
- Mayer, L.; Jakobsson, M.; Allen, G.; Dorschel, B.; Falconer, R.; Ferrini, V.; Lamarche, G.; Snaith, H.; Weatherall, P. The Nippon Foundation—GEBCO seabed 2030 project: The quest to see the world's oceans completely mapped by 2030. *Geosciences* **2018**, *8*, 63. [[CrossRef](#)]
- Wulff, U.; Wulff, T. Correcting Navigation Data of shallow-diving AUV in Arctic. *Sea Technol.* **2015**, *56*, 27–30.
- Wulff, T.; Bauerfeind, E.; von Appen, W.J. Physical and ecological processes at a moving ice edge in the Fram Strait as observed with an AUV. *Deep. Sea Res. Part I Oceanogr. Res. Pap.* **2016**, *115*, 253–264. [[CrossRef](#)]
- Jørgensen, L.; Archambault, P.; Armstrong, C.; Dolgov, A.; Edinger, E.; Gaston, T.; Hildebrand, J.; Piepenburg, D.; Smith, W.; Quillfeldt, C.; et al. Arctic marine biodiversity. In *The First Global Integrated Marine Assessment, World Ocean Assessment I*; United Nations: New York, NY, USA, 2016; p. 47.
- Boetius, A.; Albrecht, S.; Bakker, K.; Bienhold, C.; Felden, J.; Fernández-Méndez, M.; Hendricks, S.; Katlein, C.; Lalande, C.; Krumpen, T.; et al. RV Polarstern ARK27-3-Shipboard Science Party. Export of Algal Biomass from the Melting Arctic Sea Ice. *Science* **2013**, *339*, 1430–1432. [[CrossRef](#)]

12. Edwards, M.; Kurras, G.; Tolstoy, M.; Bohnenstiehl, D.; Coakley, B.; Cochran, J. Evidence of recent volcanic activity on the ultraslow-spreading Gakkel Ridge. *Nature* **2001**, *409*, 808–812. [[CrossRef](#)]
13. Fisher, R.; Goodwillie, A. The Physiography of the Southwest Indian Ridge. *Mar. Geophys. Res.* **1997**, *19*, 451–455. [[CrossRef](#)]
14. Grindlay, N.R.; Madsen, J.A.; Rommevaux-Jestin, C.; Sclater, J. A different pattern of ridge segmentation and mantle Bouguer gravity anomalies along the ultra-slow spreading Southwest Indian Ridge (15°30'E to 25E). *Earth Planet. Sci. Lett.* **1998**, *161*, 243–253. [[CrossRef](#)]
15. Dick, H.J.; Lin, J.; Schouten, H. An ultraslow-spreading class of ocean ridge. *Nature* **2003**, *426*, 405–412. [[CrossRef](#)] [[PubMed](#)]
16. Scambos, T.A.; Bell, R.E.; Alley, R.B.; Anandakrishnan, S.; Bromwich, D.H.; Brunt, K.; Christianson, K.; Creyts, T.; Das, S.B.; DeConto, R.; et al. How much, how fast? A science review and outlook for research on the instability of Antarctica's Thwaites Glacier in the 21st century. *Glob. Planet. Chang.* **2017**, *153*, 16–34. [[CrossRef](#)]
17. Barker, L.D.L.; Whitcomb, L.L. A preliminary survey of underwater robotic vehicle design and navigation for under-ice operations. In Proceedings of the 2016 IEEE/RSJ International Conference on Intelligent Robots and Systems (IROS), Daejeon, Korea, 9–14 October 2016; pp. 2028–2035. [[CrossRef](#)]
18. Straneo, F.; Hamilton, G.; Stearns, L.; Sutherland, D. Connecting the Greenland Ice Sheet and the Ocean: A Case Study of Helheim Glacier and Sermilik Fjord. *Oceanography* **2016**, *29*, 34–45. [[CrossRef](#)]
19. Joughin, I.; Shean, D.E.; Smith, B.E.; Floricioiu, D. A decade of variability on Jakobshavn Isbrae: Ocean temperatures pace speed through influence on mélange rigidity. *Cryosphere* **2020**, *14*, 211–227. [[CrossRef](#)] [[PubMed](#)]
20. Khazendar, A.; Fenty, I.G.; Carroll, D.; Gardner, A.; Lee, C.M.; Fukumori, I.; Wang, O.; Zhang, H.; Seroussi, H.; Moller, D.; et al. Interruption of two decades of Jakobshavn Isbrae acceleration and thinning as regional ocean cools. *Nat. Geosci.* **2019**, *12*, 277–283. [[CrossRef](#)]
21. IMBIE Team. Mass balance of the Greenland Ice Sheet from 1992 to 2018. *Nature* **2020**, *579*, 233–239. [[CrossRef](#)]
22. Shepherd, A.; Ivins, E.; Rignot, E.; Smith, B.; van den Broeke, M.; Velicogna, I.; Whitehouse, P.; Briggs, K.; Joughin, I.; Krinner, G.; et al. Mass balance of the Antarctic Ice Sheet from 1992 to 2017. *Nature* **2018**, *558*, 219–222. [[CrossRef](#)]
23. Jacobs, S.S.; Giulivi, C.F. Large Multidecadal Salinity Trends near the Pacific-Antarctic Continental Margin. *J. Clim.* **2010**, *23*, 4508–4524. [[CrossRef](#)]
24. Rye, C.D.; Naveira Garabato, A.C.; Holland, P.R.; Meredith, M.P.; George Nurser, a.J.; Hughes, C.W.; Coward, A.C.; Webb, D.J. Rapid sea-level rise along the Antarctic margins in response to increased glacial discharge. *Nat. Geosci.* **2014**, *7*, 732–735. [[CrossRef](#)]
25. Nicholls, K.W.; Østerhus, S.; Makinson, K.; Gammelsrød, T.; Fahrbach, E. Ice-ocean processes over the continental shelf of the southern Weddell Sea, Antarctica: A review. *Rev. Geophys.* **2009**, *47*. [[CrossRef](#)]
26. Alderkamp, A.C.; van Dijken, G.L.; Lowry, K.E.; Connelly, T.L.; Lagerström, M.; Sherrell, R.M.; Haskins, C.; Rogalsky, E.; Schofield, O.; Stammerjohn, S.E.; et al. Fe availability drives phytoplankton photosynthesis rates during spring bloom in the Amundsen Sea Polynya, Antarctica. *Elem. Sci. Anthr.* **2015**, *3*, 000043. [[CrossRef](#)]
27. Sherrell, R.; Lagerström, M.; Forsch, K.; Stammerjohn, S.; Yager, P. Dynamics of dissolved iron and other bioactive trace metals (Mn, Ni, Cu, Zn) in the Amundsen Sea Polynya, Antarctica. *Elem. Sci. Anthr.* **2015**, *3*, 000071. [[CrossRef](#)]
28. Arrigo, K.R.; van Dijken, G.; Long, M. Coastal Southern Ocean: A strong anthropogenic CO<sub>2</sub> sink. *Geophys. Res. Lett.* **2008**, *35*, 1–6. [[CrossRef](#)]
29. Nicholls, K.W.; Abrahamsen, E.P.; Buck, J.J.H.; Dodd, P.A.; Goldblatt, C.; Griffiths, G.; Heywood, K.J.; Hughes, N.E.; Kaletzky, A.; Lane-Serff, G.F.; et al. Measurements beneath an Antarctic ice shelf using an autonomous underwater vehicle. *Geophys. Res. Lett.* **2006**, *33*, 2–5. [[CrossRef](#)]
30. Jenkins, A.; Dutrieux, P.; Jacobs, S.S.; McPhail, S.D.; Perrett, J.R.; Webb, A.T.; White, D. Observations beneath Pine Island Glacier in West Antarctica and implications for its retreat. *Nat. Geosci.* **2010**, *3*, 468–472. [[CrossRef](#)]

31. Smith, J.A.; Andersen, T.J.; Shortt, M.; Gaffney, A.M.; Truffer, M.; Stanton, T.P.; Bindschadler, R.; Dutrieux, P.; Jenkins, A.; Hillenbrand, C.D.D.; et al. Sub-ice-shelf sediments record history of twentieth-century retreat of Pine Island Glacier. *Nature* **2016**, *541*, 77–80. [[CrossRef](#)]
32. Jacobs, S.S.; Jenkins, A.; Giulivi, C.F.; Dutrieux, P. Stronger ocean circulation and increased melting under Pine Island Glacier ice shelf. *Nat. Geosci.* **2011**, *4*, 519–523. [[CrossRef](#)]
33. Dutrieux, P.; De Rydt, J.; Jenkins, A.; Holland, P.R.; Ha, H.K.; Lee, S.H.; Steig, E.J.; Ding, Q.; Abrahamsen, E.P.; Schroder, M. Strong Sensitivity of Pine Island Ice-Shelf Melting to Climatic Variability. *Science* **2014**, *343*, 174–178. [[CrossRef](#)]
34. Holland, P.R.; Bracegirdle, T.J.; Dutrieux, P.; Jenkins, A.; Steig, E.J. West Antarctic ice loss influenced by internal climate variability and anthropogenic forcing. *Nat. Geosci.* **2019**, *1*–7. [[CrossRef](#)]
35. Graham, A.G.C.; Dutrieux, P.; Vaughan, D.G.; Nitsche, F.O.; Gyllencreutz, R.; Greenwood, S.L.; Larter, R.D.; Jenkins, A. Seabed corrugations beneath an Antarctic ice shelf revealed by autonomous underwater vehicle survey: Origin and implications for the history of Pine Island Glacier. *J. Geophys. Res. Earth Surf.* **2013**, *118*, 1356–1366. [[CrossRef](#)]
36. Davies, D.; Bingham, R.G.; Graham, A.G.C.; Spagnolo, M.; Dutrieux, P.; Vaughan, D.G.; Jenkins, A.; Nitsche, F.O. High-resolution sub-ice-shelf seafloor records of twentieth century ungrounding and retreat of Pine Island Glacier, West Antarctica. *J. Geophys. Res. Earth Surf.* **2017**, *122*, 1698–1714. [[CrossRef](#)]
37. Dutrieux, P.; Stewart, C.; Jenkins, A.; Nicholls, K.W.; Corr, H.F.J.; Rignot, E.; Steffen, K. Basal terraces on melting ice shelves. *Geophys. Res. Lett.* **2014**, *41*, 5506–5513. [[CrossRef](#)]
38. Dutrieux, P.; Jenkins, A.; Nicholls, K.W. Ice-shelf basal morphology from an upward-looking multibeam system deployed from an autonomous underwater vehicle. *Geol. Soc. Lond. Mem.* **2016**, *46*, 219–220. [[CrossRef](#)]
39. Dutrieux, P.; Vaughan, D.G.; Corr, H.F.J.; Jenkins, A.; Holland, P.R.; Jougin, I.; Fleming, A.H. Pine Island glacier ice shelf melt distributed at kilometre scales. *Cryosphere* **2013**, *7*, 1543–1555. [[CrossRef](#)]
40. Shean, D.E.; Jougin, I.R.; Dutrieux, P.; Smith, B.E.; Berthier, E. Ice shelf basal melt rates from a high-resolution digital elevation model (DEM) record for Pine Island Glacier, Antarctica. *Cryosphere* **2019**, *13*, 2633–2656. [[CrossRef](#)]
41. Kimura, S.; Jenkins, A.; Dutrieux, P.; Forryan, A.; Naveira Garabato, A.C.; Firing, Y. Ocean mixing beneath Pine Island Glacier ice shelf, West Antarctica. *J. Geophys. Res. Ocean.* **2016**, *121*, 8496–8510. [[CrossRef](#)]
42. Maksym, T. Arctic and Antarctic Sea Ice Change: Contrasts, Commonalities, and Causes. *Annu. Rev. Mar. Sci.* **2019**, *11*, 187–213. [[CrossRef](#)]
43. Stroeve, J.C.; Kattsov, V.; Barrett, A.; Serreze, M.; Pavlova, T.; Holland, M.; Meier, W.N. Trends in Arctic sea ice extent from CMIP5, CMIP3 and observations. *Geophys. Res. Lett.* **2012**, *39*. [[CrossRef](#)]
44. Hobbs, W.R.; Massom, R.; Stammerjohn, S.; Reid, P.; Williams, G.; Meier, W. A review of recent changes in Southern Ocean sea ice, their drivers and forcings. *Glob. Planet. Chang.* **2016**, *143*, 228–250. [[CrossRef](#)]
45. Rothrock, D.A.; Yu, Y.; Maykut, G.A. Thinning of the Arctic sea ice cover. *Geophys. Res. Lett.* **1999**, *26*, 3469–3472. [[CrossRef](#)]
46. Wadhams, P.; Davis, N.R. Further evidence of ice thinning in the Arctic Ocean. *Geophys. Res. Lett.* **2000**, *27*, 3973–3975. [[CrossRef](#)]
47. Kwok, R.; Rothrock, D.A. Decline in Arctic sea ice thickness from submarine and ICESat records: 1958–2008. *Geophys. Res. Lett.* **2009**, *36*. [[CrossRef](#)]
48. Kwok, R.; Cunningham, G.F. Variability of Arctic sea ice thickness and volume from CryoSat-2. *Philos. Trans. R. Soc. A Math. Phys. Eng. Sci.* **2015**, *373*, 20140157. [[CrossRef](#)] [[PubMed](#)]
49. Wadhams, P.; Wilkinson, J.P.; McPhail, S.D. A new view of the underside of Arctic sea ice. *Geophys. Res. Lett.* **2006**, *33*, 1–5. [[CrossRef](#)]
50. Williams, G.; Maksym, T.; Wilkinson, J.; Kunz, C.; Murphy, C.; Kimball, P.; Singh, H. Thick and deformed Antarctic sea ice mapped with autonomous underwater vehicles. *Nat. Geosci.* **2015**, *8*, 61–67. [[CrossRef](#)]
51. Mei, M.J.; Maksym, T.; Weissling, B.; Singh, H. Estimating early-winter Antarctic sea ice thickness from deformed ice morphology. *Cryosphere* **2019**, *13*, 2915–2934. [[CrossRef](#)]
52. Kwok, R.; Markus, T.; Kurtz, N.T.; Petty, A.A.; Neumann, T.A.; Farrell, S.L.; Cunningham, G.F.; Hancock, D.W.; Ivanoff, A.; Wimert, J.T. Surface Height and Sea Ice Freeboard of the Arctic Ocean From ICESat-2: Characteristics and Early Results. *J. Geophys. Res. Ocean.* **2019**, *124*, 6942–6959. [[CrossRef](#)]

53. Carmack, E.; Polyakov, I.; Padman, L.; Fer, I.; Hunke, E.; Hutchings, J.; Jackson, J.; Kelley, D.; Kwok, R.; Layton, C.; et al. Toward Quantifying the Increasing Role of Oceanic Heat in Sea Ice Loss in the New Arctic. *Bull. Am. Meteorol. Soc.* **2015**, *96*, 2079–2105. [[CrossRef](#)]
54. Polyakov, I.V.; Pnyushkov, A.V.; Alkire, M.B.; Ashik, I.M.; Baumann, T.M.; Carmack, E.C.; Gosczko, I.; Guthrie, J.; Ivanov, V.V.; Kanzow, T.; et al. Greater role for Atlantic inflows on sea ice loss in the Eurasian Basin of the Arctic Ocean. *Science* **2017**, *356*, 285–291. [[CrossRef](#)]
55. Woodgate, R.A.; Weingartner, T.; Lindsay, R. The 2007 Bering Strait oceanic heat flux and anomalous Arctic sea ice retreat. *Geophys. Res. Lett.* **2010**, *37*. [[CrossRef](#)]
56. Jackson, J.M.; Williams, W.J.; Carmack, E.C. Winter sea ice melt in the Canada Basin, Arctic Ocean. *Geophys. Res. Lett.* **2012**, *39*. [[CrossRef](#)]
57. Timmermans, M.L.; Toole, J.; Krishfield, R. Warming of the interior Arctic Ocean linked to sea ice losses at the basin margins. *Sci. Adv.* **2018**, *4*. [[CrossRef](#)] [[PubMed](#)]
58. Thomson, J.; Rogers, W.E. Swell and sea in the emerging Arctic Ocean. *Geophys. Res. Lett.* **2014**, *41*, 3136–3140. [[CrossRef](#)]
59. Freitag, L.; Ball, K.; Partan, J.; Koski, P.; Singh, S. Long range acoustic communications and navigation in the Arctic. In Proceedings of the OCEANS 2015—MTS/IEEE Washington, Washington, DC, USA, 19–22 October 2015; pp. 1–5.
60. Lecomte, O.; Goosse, H.; Fichefet, T.; de Lavergne, C.; Barthélémy, A.; Zunz, V. Vertical ocean heat redistribution sustaining sea ice concentration trends in the Ross Sea. *Nat. Commun.* **2017**, *8*, 258. [[CrossRef](#)] [[PubMed](#)]
61. Meehl, G.A.; Arblaster, J.M.; Chung, C.T.Y.; Holland, M.M.; DuVivier, A.; Thompson, L.; Yang, D.; Bitz, C.M. Sustained ocean changes contributed to sudden Antarctic sea ice retreat in late 2016. *Nat. Commun.* **2019**, *10*. [[CrossRef](#)]
62. Squire, V.A. The marginal ice zone. In *Physics of Ice-Covered Seas*; Lepparanta, M., Ed.; Helsinki University Printing House: Helsinki, Finland, 1998; Volume 1, pp. 281–446.
63. Ackley, S.F.; Stammerjohn, S.; Maksym, T.; Smith, M.; Cassano, J.; Guest, P.; Tison, J.L.; Delille, B.; Loose, B.; Sedwick, P.; et al. Sea ice production and air-ice-ocean-biogeochemistry interactions in the Ross Sea during the PIPERS 2017 autumn field campaign. *Ann. Glaciol.* **2020**, in press. [[CrossRef](#)]
64. Bronwyn, W. A drift in the Arctic. *Nat. Clim. Chang.* **2019**, *9*, 733. [[CrossRef](#)]
65. Lee, C.M.; Thomson, J. An autonomous approach to observing the seasonal ice zone in the western Arctic Oceanography. *Oceanography* **2016**, *30*, 56–68. [[CrossRef](#)]
66. Lee, C.M.; Cole, S.; Doble, M.; Guthrie, J.D.; Mackinnon, J.; Morison, J.; Musgrave, R.; Peacock, T.; Rainville, L.; Stanton, T.; et al. *Stratified Ocean Dynamics of the Arctic: Science and Experiment Plan*; Technical Report APL-UW 1601; Applied Physics Laboratory, University of Washington: Seattle, WA, USA, 2016.
67. Newman, L.; Heil, P.; Trebilco, R.; Katsumata, K.; Constable, A.; van Wijk, E.; Assmann, K.; Beja, J.; Bricher, P.; Coleman, R.; et al. Delivering Sustained, Coordinated, and Integrated Observations of the Southern Ocean for Global Impact. *Front. Mar. Sci.* **2019**, *6*, 433. [[CrossRef](#)]
68. Raskoff, K.; Hopcroft, R.; Kosobokova, K.; Purcell, J.; Youngbluth, M. Jellies under ice: ROV observations from the Arctic 2005 hidden ocean expedition. *Deep. Sea Res. Part II Top. Stud. Oceanogr.* **2010**, *57*, 111–126. [[CrossRef](#)]
69. Katlein, C.; Schiller, M.; Belter, H.J.; Coppolaro, V.; Wenslandt, D.; Nicolaus, M. A New Remotely Operated Sensor Platform for Interdisciplinary Observations under Sea Ice. *Front. Mar. Sci.* **2017**, *4*, 281. [[CrossRef](#)]
70. German, C.R.; Boetius, A.; Whitcomb, L.L.; Jakuba, M.; Bailey, J.; Judge, C.; McFarland, C.; Suman, S.; Elliott, S.; Katlein, C.; et al. *First Scientific Dives of the Nereid Under Ice Hybrid ROV in the Arctic Ocean*; AGU Fall Meeting Abstracts: San Francisco, CA, USA, 2014; Volume 2014, abstract ID B23G–07. Available online: <https://ui.adsabs.harvard.edu/abs/2014AGUFM.B23G..07G> (accessed on 30 June 2020).
71. Gutt, J.; Piepenburg, D. Scale-dependent impact on diversity of Antarctic benthos caused by grounding of icebergs. *Mar. Ecol. Prog. Ser.* **2003**, *253*, 77–83. [[CrossRef](#)]
72. Soltwedel, T.; Hasemann, C.; Vedenin, A.; Bergmann, M.; Taylor, J.; Krauß, F. Bioturbation rates in the deep Fram Strait: Results from in situ experiments at the arctic LTER observatory HAUSGARTEN. *J. Exp. Mar. Biol. Ecol.* **2019**, *511*, 1–9. [[CrossRef](#)]

73. Dahle, H.; Le Moine Bauer, S.; Baumberger, T.; Stokke, R.; Pedersen, R.B.; Thorseth, I.H.; Steen, I.H. Energy landscapes in hydrothermal chimneys shape distributions of primary producers. *Front. Microbiol.* **2018**, *9*, 1570. [[CrossRef](#)] [[PubMed](#)]
74. Sohn, R.A.; Willis, C.; Humphris, S.; Shank, T.M.; Singh, H.; Edmonds, H.N.; Kunz, C.; Hedman, U.; Helmke, E.; Jakuba, M.; et al. Explosive volcanism on the ultraslow-spreading Gakkel ridge, Arctic Ocean. *Nature* **2008**, *453*, 1236–1238. [[CrossRef](#)]
75. Pontbriand, C.W.; Soule, S.A.; Sohn, R.A.; Humphris, S.E.; Kunz, C.; Singh, H.; Nakamura, K.; Jakobsson, M.; Shank, T. Effusive and explosive volcanism on the ultraslow-spreading Gakkel Ridge, 85°E. *Geochim. Geophys. Geosyst.* **2012**, *13*. [[CrossRef](#)]
76. Kintisch, E. Arctic researchers prepare to go with the floes. *Science* **2019**, *365*, 728–729. [[CrossRef](#)]
77. Sommerfeld, A.; Rex, M.; Shupe, M.; Dethloff, K. The Multidisciplinary drifting Observatory for the Study of Arctic Climate (MOSAiC). In Proceedings of the EGU General Assembly Conference Abstracts, Vienna, Austria, 23–28 April 2017; p. 2115. Available online: <https://ui.adsabs.harvard.edu/abs/2017EGUGA..19.2115S> (accessed on 30 June 2020).
78. Mayer, L.A.; Armstrong, A.; Calder, B.; Gardner, J. Sea Floor Mapping in the Arctic: Support for a Potential US Extended Continental Shelf. *Int. Hydrogr. Rev.* **2010**, *3*, 14–23.
79. Straneo, F.; Heimbach, P. North Atlantic warming and the retreat of Greenland’s outlet glaciers. *Nature* **2013**, *504*, 36–43. [[CrossRef](#)]
80. Schaffer, J.; Kanzow, T.; von Appen, W.J.; von Albedyll, L.; Arndt, J.E.; Roberts, D.H. Bathymetry constrains ocean heat supply to Greenland’s largest glacier tongue. *Nat. Geosci.* **2020**, *13*, 227–231. [[CrossRef](#)]
81. Jakobsson, M.; Hogan, K.A.; Mayer, L.A.; Mix, A.; Jennings, A.; Stoner, J.; Eriksson, B.; Jerram, K.; Mohammad, R.; Pearce, C.; et al. The Holocene retreat dynamics and stability of Petermann Glacier in northwest Greenland. *Nat. Commun.* **2018**, *9*, 2104. [[CrossRef](#)] [[PubMed](#)]
82. Jakobsson, M.; Nilsson, J.; Anderson, L.; Backman, J.; Björk, G.; Cronin, T.M.; Kirchner, N.; Koshurnikov, A.; Mayer, L.; Noormets, R.; et al. Evidence for an ice shelf covering the central Arctic Ocean during the penultimate glaciation. *Nat. Commun.* **2016**, *7*, 10365. [[CrossRef](#)] [[PubMed](#)]
83. Thorsnes, T.; Brunstad, H.; Lågstad, P.; Chand, S. Trawl marks, iceberg ploughmarks and possible whale-feeding marks, Barents Sea. *Geol. Soc. Lond. Mem.* **2016**, *46*, 293–294. [[CrossRef](#)]
84. Gausepohl, F.; Hennke, A.; Schoening, T.; Köser, K.; Greinert, J. Scars in the abyss: Reconstructing sequence, location and temporal change of the 78 plough tracks of the 1989 DISCOL deep-sea disturbance experiment in the Peru Basin. *Biogeosciences* **2020**, *17*, 1463–1493. [[CrossRef](#)]
85. Toole, J.; Krishfield, R.; Proshutinsky, A.; Ashjian, C.; Doherty, K.; Frye, D.; Hammar, T.; Kemp, J.; Peters, D.; Timmermans, M.L.; et al. Ice-tethered profilers sample the upper Arctic Ocean. *Eos. Trans. Am. Geophys. Union* **2006**, *87*, 434–438. [[CrossRef](#)]
86. Brumley, K.; Mayer, L.A.; Miller, E.; Coakley, B. Dredged rock samples from the Alpha Ridge, Arctic Ocean: Implications for the tectonic history and origin of the Amerasia Basin. *Eos. Trans. AGU* **2008**, *89*, T43B-2013.
87. Lawver, L.; Scotese, C. A review of tectonic models for the evolution of the Canada Basin. *Geol. N. Am.* **1990**, *50*, 593–618.
88. Grantz, A.; Hart, P.E.; Childers, V.A. Chapter 50 Geology and tectonic development of the Amerasia and Canada Basins, Arctic Ocean. *Geol. Soc. Lond. Mem.* **2011**, *35*, 771–799. [[CrossRef](#)]
89. Døssing, A.; Jackson, H.; Matzka, J.; Einarsson, I.; Rasmussen, T.; Olesen, A.; Brozena, J. On the origin of the Amerasia Basin and the High Arctic Large Igneous Province—Results of new aeromagnetic data. *Earth Planet. Sci. Lett.* **2013**, *363*, 219–230. [[CrossRef](#)]
90. Chernykh, A.; Glebovsky, V.; Zykov, M.; Korneva, M. New insights into tectonics and evolution of the Amerasia Basin. *J. Geodyn.* **2018**, *119*, 167–182. [[CrossRef](#)]
91. Mukasa, S.; Andronikov, A.; Mayer, L.; Brumley, K. Submarine basalts from the Alpha/Mendeleev Ridge and Chukchi Borderland: Geochemistry of the first intraplate lavas recovered from the Arctic Ocean. *Geochim. Cosmochim. Acta Suppl.* **2009**, *73*, A912.
92. Ferran, C.G. The Bransfield rift and its active volcanism. In *Geological Evolution of Antarctica*; Thomson, M., Crame, J., Thomson, J., Eds.; Cambridge University Press: Cambridge, UK, 1991; pp. 505–509.
93. Lawver, L.A.; Sloan, B.J.; Barker, D.H.; Ghidella, M.; Von Herzen, R.P.; Keller, R.A.; Klinkhammer, G.P.; Chin, C.S. Distributed, active extension in Bransfield Basin, Antarctic Peninsula: Evidence from multibeam bathymetry. *GSA Today* **1996**, *6*, 1–6.

94. Gràcia, E.; Canals, M.; Farràn, M.L.; Prieto, M.J.; Sorribas, J.; Team, G. Morphostructure and evolution of the central and eastern Bransfield basins (NW Antarctic Peninsula). *Mar. Geophys. Res.* **1996**, *18*, 429–448. [\[CrossRef\]](#)
95. Klinkhammer, G.; Chin, C.; Keller, R.; Dähmann, A.; Sahling, H.; Sarthou, G.; Petersen, S.; Smith, F.; Wilson, C. Discovery of new hydrothermal vent sites in Bransfield Strait, Antarctica. *Earth Planet. Sci. Lett.* **2001**, *193*, 395–407. [\[CrossRef\]](#)
96. Barker, D.H.; Christeson, G.L.; Austin Jr, J.A.; Dalziel, I.W. Backarc basin evolution and cordilleran orogenesis: Insights from new ocean-bottom seismograph refraction profiling in Bransfield Strait, Antarctica. *Geology* **2003**, *31*, 107–110. [\[CrossRef\]](#)
97. Michael, P.; Langmuir, C.; Dick, H.; Snow, J.; Goldstein, S.; Graham, D.; Lehnert, K.; Kurras, G.; Jokat, W.; Mühe, R.; et al. Magmatic and amagmatic seafloor generation at the ultraslow-spreading Gakkel ridge, Arctic Ocean. *Nature* **2003**, *423*, 956–961. [\[CrossRef\]](#)
98. Hendrix, A.R.; Hurford, T.A.; Barge, L.M.; Bland, M.T.; Bowman, J.S.; Brinckerhoff, W.; Buratti, B.J.; Cable, M.L.; Castillo-Rogez, J.; Collins, G.C.; et al. The NASA Roadmap to Ocean Worlds. *Astrobiology* **2019**, *19*, 1–27. [\[CrossRef\]](#)
99. Kinsey, J.C.; Eustice, R.M.; Whitcomb, L.L. A survey of underwater vehicle navigation: Recent advances and new challenges. In Proceedings of the IFAC Conference of Manoeuvering and Control of Marine Craft, Lisbon, Portugal, 20–22 September 2006; Volume 88.
100. Francois, R.E.; Nodland, W.E. *Unmanned Arctic Research Submersible UARS System Development and Test Report*; Technical Report APL-UW 7219; University of Washington, Applied Physics Laboratory: Seattle, WA, USA, 1972.
101. Francois, R.E. *High Resolution Observations of Under-Ice Morphology*; Technical Report APL-UW 7712; University of Washington, Applied Physics Laboratory: Seattle, WA, USA, 1977.
102. Deffenbaugh, M.; Schmidt, H.; Bellingham, J.G. Acoustic Navigation for Arctic under-ice AUV missions. In Proceedings of the IEEE/MTS Oceans Conference and Exhibition, Victoria, BC, Canada, 18–21 October 1993; Volume 1, pp. 1204–1209.
103. McEwen, R.; Thomas, H.; Weber, D.; Psota, F. Performance of an AUV navigation system at Arctic latitudes. *IEEE J. Ocean. Eng.* **2005**, *30*, 443–454. [\[CrossRef\]](#)
104. Thorleifson, J.; Davies, T.; Black, M.; Hopkin, D.; Verrall, R. The Theseus Autonomous Underwater Vehicle: A Canadian Success Story. In Proceedings of the IEEE/MTS Oceans Conference and Exhibition, Halifax, NS, Canada, 6–9 October 1997; pp. 1001–1008.
105. Kaminski, C.; Crees, T.; Ferguson, J.; Forrest, A.; Williams, J.; Hopkin, D.; Heard, G. 12 days under ice—An historic AUV deployment in the Canadian High Arctic. In Proceedings of the 2010 IEEE/OES Autonomous Underwater Vehicles, Monterey, CA, USA, 1–3 September 2010; pp. 1–11, [\[CrossRef\]](#)
106. Crees, T.; Kaminski, C.; Ferguson, J.; Laframboise, J.M.; Forrest, A.; Williams, J.; MacNeil, E.; Hopkin, D.; Pederson, R. UNCLOS under ice survey—An historic AUV deployment in the Canadian high arctic. In Proceedings of the OCEANS 2010 MTS/IEEE SEATTLE, Seattle, WA, USA, 20–23 September 2010; pp. 1–8, [\[CrossRef\]](#)
107. Eustice, R.M.; Whitcomb, L.L.; Singh, H.; Grund, M. Recent Advances in Synchronous-Clock One-Way-Travel-Time Acoustic Navigation. In Proceedings of the IEEE/MTS Oceans Conference and Exhibition, Boston, MA, USA, 18–21 September 2006.
108. Jakuba, M.V.; Roman, C.N.; Singh, H.; Murphy, C.; Kunz, C.; Willis, C.; Sato, T.; Sohn, R.A. Long-baseline acoustic navigation for under-ice autonomous underwater vehicle operations. *J. Field Robot.* **2008**, *25*, 861–879. [\[CrossRef\]](#)
109. McFarland, C.; Jakuba, M.; Suman, S.; Kinsey, J.; Whitcomb, L. Toward ice-relative navigation of underwater robotic vehicles under moving sea ice: Experimental evaluation in the Arctic Sea. In Proceedings of the 2015 IEEE International Conference on Robotics and Automation (ICRA), Seattle, WA, USA, 26–30 May 2015; pp. 1527–1534. [\[CrossRef\]](#)
110. Francois, R.E. The Unmanned Arctic Research Submersible System. *Mar. Technol. Soc. J.* **1973**, *7*, 46–48. [\[CrossRef\]](#)
111. Brooke, J. ARCS (Autonomous remotely controlled submersible). In Proceedings of the International Symposium of Unmanned Untethered Submersible Technology, Boston, MA, USA, 21–24 September 1981; p. 28.

112. Jackson, E. Autonomous remotely controlled submersible “ARCS”. In Proceedings of the 1983 3rd International Symposium on Unmanned Untethered Submersible Technology, Durham, NH, USA, 6–9 June 1983; Volume 3, pp. 77–88. [[CrossRef](#)]
113. Thomas, B. Control software in the ARCS vehicle. In Proceedings of the International Symposium of Unmanned Untethered Submersible Technology, Durham, NH, USA, 6–9 June 1985; Volume 4, pp. 334–342. [[CrossRef](#)]
114. Light, R.D.; Morison, J. The Autonomous Conductivity-Temperture Vehicle: First in the Seashuttle Family of Autonomous Underwater Vehicle’s for Scientific Payloads. In Proceedings of the IEEE/MTS Oceans Conference and Exhibition, Seattle, WA, USA, 18–21 September 1989; pp. 793–798.
115. Nicholls, K.W.; Abrahamsen, E.P.; Heywood, K.J.; Stansfield, K.; Østerhus, S. High-latitude oceanography using the Autosub autonomous underwater vehicle. *Limnol. Oceanogr.* **2008**, *53*, 2309–2320. [[CrossRef](#)]
116. McPhail, S.; Furlong, M.; Pebody, M.; Perrett, J.; Stevenson, P.; Webb, A.; White, D. Exploring beneath the PIG Ice Shelf with the Autosub3 AUV. In Proceedings of the IEEE/MTS Oceans Conference and Exhibition, Bremen, Germany, 11–14 May 2009; pp. 1–8. [[CrossRef](#)]
117. McPhail, S.; Templeton, R.; Pebody, M.; Roper, D.; Morrison, R. Autosub Long Range AUV Missions Under the Filchner and Ronne Ice Shelves in the Weddell Sea, Antarctica—An Engineering Perspective. In Proceedings of the OCEANS 2019-Marseille, Marseille, France, 17–20 June 2019; IEEE: New York, NY, USA, 2019; pp. 1–8.
118. Forrest, A.; Bohm, H.; Laval, B.; Magnusson, E.; Yeo, R.; Doble, M. Investigation of under-ice thermal structure: Small AUV deployment in Pavilion Lake, BC, Canada. In Proceedings of the IEEE/MTS Oceans Conference and Exhibition, Vancouver, BC, Canada, 29 September–4 October 2007; pp. 1–9. [[CrossRef](#)]
119. Forrest, A.; Hamilton, A.; Schmidt, V.; Laval, B.; Mueller, D.; Crawford, A.; Brucker, S.; Hamilton, T. Digital terrain mapping of Petermann Ice Island fragments in the Canadian High Arctic. In Proceedings of the 21st IAHR International Symposium on Ice, Dalian, China, 11–15 June 2012; pp. 1–12.
120. Doble, M.J.; Forrest, A.L.; Wadhams, P.; Laval, B.E. Through-ice AUV deployment: Operational and technical experience from two seasons of Arctic fieldwork. *Cold Reg. Sci. Technol.* **2009**, *56*, 90–97. [[CrossRef](#)]
121. Wadhams, P. The use of autonomous underwater vehicles to map the variability of under-ice topography. *Ocean Dyn.* **2012**, *62*, 439–447. [[CrossRef](#)]
122. Stone, W.C.; Hogan, B.; Flesher, C.; Gulati, S.; Richmond, K.; Murarka, A.; Kuhlman, G.; Sridharan, M.; Siegel, V.; Price, R.M.; et al. Sub-ice exploration of West Lake Bonney: ENDURANCE 2008 Mission. In Proceedings of the International Symposium on Unmanned Untethered Submersible Technology 2009 (UUST 2009), Durham, NH, USA, 23–26 August 2009.
123. Richmond, K.; Febretti, A.; Gulati, S.; Flesher, C.; Hogan, B.P.; Murarka, A.; Kuhlman, G.; Sridharan, M.; Johnson, A.; Stone, W.C.; et al. Sub-Ice Exploration of an Antarctic Lake: Results from the ENDURANCE Project. In Proceedings of the International Symposium of Unmanned Untethered Submersible Technology, Portsmouth, NH, USA, 21–24 August 2011.
124. Kukulya, A.; Plueddemann, A.; Austin, T.; Stokey, R.; Purcell, M.; Allen, B.; Littlefield, R.; Freitag, L.; Koski, P.; Gallimore, E.; et al. Under-ice operations with a REMUS-100 AUV in the Arctic. In Proceedings of the IEEE/OES Autonomous Underwater Vehicles (AUV), Monterey, CA, USA, 1–3 September 2010; IEEE: New York, NY, USA, 2010; pp. 1–8.
125. Hildebrandt, M.; Albiez, J.; Fritzsche, M.; Hilljegerdes, J.; Kloss, P.; Wirtz, M.; Kirchner, F. Design of an autonomous under-ice exploration system. In Proceedings of the IEEE/MTS Oceans Conference and Exhibition, San Diego, CA, USA, 23–27 September 2013; pp. 1–6.
126. Forrest, A.L.; Lund-Hansen, L.C.; Sorrell, B.K.; Bowden-Floyd, I.; Lucieer, V.; Cossu, R.; Lange, B.A.; Hawes, I. Exploring Spatial Heterogeneity of Antarctic Sea Ice Algae Using an Autonomous Underwater Vehicle Mounted Irradiance Sensor. *Front. Earth Sci.* **2019**, *7*, 169. [[CrossRef](#)]
127. Spain, E.; Gwyther, D.; King, P. Submarine ventures under Sørdsdal Glacier. *Aust. Antarct. Mag.* **2019**, *18*.
128. Beeler, C. One Year into the Mission, Autonomous Ocean Robots Set a Record in Survey of Antarctic Ice Shelf. Available online: <https://www.pri.org/stories/2019-03-06/antarctica-dispatch-7-under-thwaites-glacier> (accessed on 6 March 2019).
129. Hobson, B.; Raanan, B.Y. Personal communication to first Author, 25 February 2020.

130. Bono, R.; Bruzzone, G.; Caccia, M.; Grassia, F.; Spirandelli, E.; Veruggio, G. ROBY goes to Antarctica. In Proceedings of the IEEE/MTS Oceans Conference and Exhibition, Brest, France, 13–16 September 1994; Volume 3, pp. 621–625. [[CrossRef](#)]
131. Veruggio, G.; Bono, R.; Caccia, M. The control system of a small virtual AUV. In Proceedings of the Symposium on Autonomous Underwater Vehicle Technology, Cambridge, MA, USA, 19–20 July 1994; pp. 69–74. [[CrossRef](#)]
132. Stoker, C.R.; Barch, D.R.; Hine III, B.P.; Barry, J. Antarctic undersea exploration using a robotic submarine with a telepresence user interface. *IEEE Expert* **1995**, *10*, 14–23. [[CrossRef](#)]
133. Caccia, M.; Bono, R.; Bruzzone, G.; Veruggio, G. Variable-configuration UUVs for marine science applications. *IEEE Robot. Autom. Mag.* **1999**, *6*, 22–32. [[CrossRef](#)]
134. Vogel, S.W.; Powell, R.D.; Griffith, I.; Anderson, K.; Lawson, T.; Schiraga, S.A. Subglacial environment exploration—Concept and technological challenges for the development and operation of a Sub-Ice ROV'er (SIR) and advanced Sub-Ice instrumentation for short and long-term observations. In Proceedings of the IEEE/OES Autonomous Underwater Vehicles, AUV 2008, Woods Hole, MA, USA, 13–14 October 2008; p. 3. [[CrossRef](#)]
135. Cazenave, F.; Zook, R.; Carroll, D.; Flagg, M.; Kim, S. The skinny on SCINI. *J. Ocean. Technol.* **2011**, *6*, 39–58.
136. SCINI Deployment Procedures (2012–2015), 2015.
137. Behar, A.E.; Chen, D.D.; Ho, C.; McBryan, E.; Walter, C.; Horen, J.; Foster, S.; Foster, T.; Warren, A.; Vemprala, S.H.; et al. MSLED: The Micro Subglacial Lake Exploration Device. *Underw. Technol.* **2015**, *33*, 3–17. [[CrossRef](#)]
138. Burnett, J.; Rack, F.; Zook, R.; Schmidt, B. Development of a Borehole Deployable Remotely Operated Vehicle for Investigation of Sub-Ice Aquatic Environments. In Proceedings of the IEEE/MTS Oceans Conference and Exhibition, Washington, DC, USA, 19–22 October 2015.
139. Spears, A.; Howard, A.; Schmidt, B.; Meister, M.; West, M.; Collins, T. Design and development of an under-ice autonomous underwater vehicle for use in Polar regions. In Proceedings of the IEEE/MTS Oceans Conference and Exhibition, St. John's, NL, Canada, 14–19 September 2014; pp. 1–6. [[CrossRef](#)]
140. Meister, M.; Dichek, D.; Spears, A.; Hurwitz, B.; Ramey, C.; Lawrence, J.; Philleo, K.; Lutz, J.; Lawrence, J.; Schmidt, B.E. Icefin: Redesign and 2017 Antarctic Field Deployment. In Proceedings of the OCEANS 2018 MTS/IEEE Charleston, Charleston, SC, USA, 22–25 October 2018; pp. 1–5.
141. Schmidt, B.; Spears, A. Personal communication to first Author, 20 April 2020.
142. Berisford, D.F.; Leichty, J.; Klesh, A.; Hand, K.P. *Remote Under-Ice Roving in Alaska with the Buoyant Rover for Under-Ice Exploration*; AGU Fall Meeting Abstracts: San Francisco, CA, USA, 2013; Volume 2013, abstract ID C13C-0684.
143. Aquatic Rover Goes for a Drive Under the Ice. Available online: <https://www.jpl.nasa.gov/news/news.php?feature=7543> (accessed on 18 March 2020).
144. Clark, E. Our Biggest Day Yet. 2015. Available online: <http://artemis2015.weebly.com/expedition-log/our-biggest-day-yet> (accessed on 28 January 2016).
145. Ferguson, J.; Pope, A.; Butler, B.; Verrall, R. Theseus AUV-two record breaking missions. *Sea Technol.* **1999**, *40*, 65–70.
146. Butler, B.; Verrall, R. Precision Hybrid Inertial/Acoustic Navigation System for a Long-Range Autonomous Underwater Vehicle. *Navigation* **2001**, *48*, 1–12. [[CrossRef](#)]
147. Bellingham, J.G.; Leonard, J.J.; Vaganay, J.; Goudey, C.A.; Atwood, D.K.; Consi, T.R.; Bales, J.W.; Schmidt, H.; Chrysostomidis, C. AUV Operations in the Arctic. In Proceedings of the International Symposium of Unmanned Untethered Submersible Technology, Durham, NH, USA, 12–14 June 1993; pp. 1–9.
148. Hayes, D.; Morison, J. Determining Turbulent Vertical Velocity, and Fluxes of Heat and Salt with an Autonomous Underwater Vehicle. *J. Atmos. Ocean. Technol.* **2002**, *19*, 759–779. [[CrossRef](#)]
149. Wadhams, P.; Wilkinson, J.; Kaletzky, A. Sidescan sonar imagery of the Winter Marginal Ice Zone obtained from an AUV. *J. Atmos. Ocean. Technol.* **2004**, *21*, 1462–1470. [[CrossRef](#)]
150. Brierley, A.S.; Fernandes, P.G.; Brandon, M.A.; Armstrong, F.; Millard, N.W.; McPhail, S.D.; Stevenson, P.; Pebody, M.; Perrett, J.; Squires, M.; et al. An investigation of avoidance by Antarctic krill of RRS James Clark Ross using the Autosub-2 autonomous underwater vehicle. *Fish. Res.* **2002**, *60*, 569–576. [[CrossRef](#)]

151. Kunz, C.; Murphy, C.; Singh, H.; Pontbriand, C.; Sohn, R.A.; Singh, S.; Sato, T.; Roman, C.; Nakamura, K.i.; Jakuba, M.; et al. Toward exoplanetary under-ice exploration: Robotic steps in the Arctic. *J. Field Robot.* **2009**, *26*, 411–429. [[CrossRef](#)]
152. Kimball, P.; Rock, S. Sonar-based iceberg-relative navigation for autonomous underwater vehicles. *Deep. Sea Res. Part II* **2011**, *58*, 1301–1310. [[CrossRef](#)]
153. Jalving, B.; Faugstadmo, J.E.; Vestgard, K.; Hegrenæs, O.; Engelhardt, O.; Hyland, B. Payload sensors, navigation and risk reduction for AUV under ice surveys. In Proceedings of the 2008 IEEE/OES Autonomous Underwater Vehicles, Woods Hole, MA, USA, 13–14 October 2008; pp. 1–8. [[CrossRef](#)]
154. Ferguson, J. Under-ice seabed mapping with AUVs. In Proceedings of the IEEE/MTS Oceans Conference and Exhibition, Bremen, Germany, 11–14 May 2009; pp. 1–6. [[CrossRef](#)]
155. Wadhams, P.; Doble, M.J. Digital terrain mapping of the underside of sea ice from a small AUV. *Geophys. Res. Lett.* **2008**, *35*. [[CrossRef](#)]
156. Wulff, T.; Lehmenhecker, S.; Hoge, U. Development and operation of an AUV-based water sample collector. *Sea Technol.* **2010**, *51*, 15–19.
157. Wulff, T.; Lehmenhecker, S.; Bauerfeind, E.; Hoge, U.; Shurn, K.; Klages, M. Biogeochemical research with an Autonomous Underwater Vehicle: Payload structure and Arctic operations. In Proceedings of the 2013 MTS/IEEE OCEANS-Bergen, Bergen, Norway, 10–14 June 2013; pp. 1–10.
158. Wulff, T. Physics and Ecology in the Marginal Ice Zone of the Fram Strait—A Robotic Approach. Ph.D. Thesis, University of Bremen, Bremen, Germany, 2016.
159. McEwen, R.S.; Rock, S.P.; Hobson, B. Iceberg Wall Following and Obstacle Avoidance by an AUV. In Proceedings of the 2018 IEEE/OES Autonomous Underwater Vehicle Workshop (AUV), Porto, Portugal, 6–9 November 2018; pp. 1–8.
160. Hopcroft, R. Pelagic ROV Dive. 2002. Available online: <https://oceanexplorer.noaa.gov/explorations/02arctic/logs/aug22/aug22.html> (accessed on 2 February 2016).
161. Hobson, B.W.; Sherman, A.D.; McGill, P.R. Imaging and sampling beneath free-drifting icebergs with a remotely operated vehicle. *Deep. Sea Res. Part II Top. Stud. Oceanogr.* **2011**, *58*, 1311–1317. [[CrossRef](#)]
162. Nicolaus, M.; Katlein, C. Mapping radiation transfer through sea ice using a remotely operated vehicle (ROV). *Cryosphere* **2013**, *7*, 763–777. [[CrossRef](#)]
163. Lange, B.A.; Katlein, C.; Nicolaus, M.; Peeken, I.; Flores, H. Sea ice algae chlorophyll a concentrations derived from under-ice spectral radiation profiling platforms. *J. Geophys. Res. Ocean.* **2016**, *121*, 8511–8534. [[CrossRef](#)]
164. Arndt, S.; Meiners, K.M.; Ricker, R.; Krumpen, T.; Katlein, C.; Nicolaus, M. Influence of snow depth and surface flooding on light transmission through Antarctic pack ice. *J. Geophys. Res. Ocean.* **2017**, *122*, 2108–2119. [[CrossRef](#)]
165. Jakuba, M.V.; German, C.R.; Bowen, A.D.; Whitcomb, L.L.; Hand, K.; Branch, A.; Chien, S.; McFarland, C. Teleoperation and robotics under ice: Implications for planetary exploration. In Proceedings of the 2018 IEEE Aerospace Conference, Big Sky, MT, USA, 3–10 March 2018; IEEE: New York, NY, USA, 2018; pp. 1–14.
166. Katlein, C.; Arndt, S.; Nicolaus, M.; Perovich, D.K.; Jakuba, M.V.; Suman, S.; Elliott, S.; Whitcomb, L.L.; McFarland, C.J.; Gerdes, R.; et al. Influence of ice thickness and surface properties on light transmission through Arctic sea ice. *J. Geophys. Res. Ocean.* **2015**, *120*, 5932–5944. [[CrossRef](#)]
167. Zeng, J.; Li, S.; Li, Y.; Wang, X.; Chen, Q.; Lei, R.; Li, T. The observation of sea ice in the six Chinese National Arctic Expedition using Polar-ARV. In Proceedings of the IEEE/MTS Oceans Conference and Exhibition, Washington, DC, USA, 19–22 October 2015; pp. 1–4.
168. Jenkins, S.A.; Humphreys, D.E.; Sherman, J.; Osse, J.; Jones, C.; Leonard, N.; Graver, J.; Bachmayer, R.; Clem, T.; Carroll, P.; et al. *Underwater Glider System Study: Scripps Institution of Oceanography Technical Report No. 53*; Technical Report; Scripps Institution of Oceanography: La Jolla, CA, USA, 2003.
169. Claus, B.; Bachmayer, R. Energy optimal depth control for long range underwater vehicles with applications to a hybrid underwater glider. *Auton. Robot.* **2016**, *40*, 1307–1320. [[CrossRef](#)]
170. Jones, C.; Webb, D.; Glenn, S.; Schofield, O.; Kerfoot, J.; Kohut, J.; Aragon, D.; Haldeman, C.; Haskin, T.; Kahl, A.; et al. Slocum Glider Expanding the Capabilities. In Proceedings of the 17th International Symposium on Unmanned Untethered Submersible Technology 2011 (UUST 2011), Portsmouth, NH, USA, 21–24 August 2011.

171. Zhou, M.; Bachmayer, R.; deYoung, B. Mapping the underside of an iceberg with a modified underwater glider. *J. Field Robot.* **2019**, *36*, 1102–1117. [[CrossRef](#)]
172. Webster, S.E.; Lee, C.M.; Gobat, J.I. Preliminary Results in Under-Ice Acoustic Navigation for Seagliders in Davis Strait. In Proceedings of the IEEE/MTS Oceans Conference and Exhibition, St. John's, NL, Canada, 14–19 September 2014; pp. 1–5.
173. Webster, S.; Freitag, L.; Lee, C.; Gobat, J. Towards real-time under-ice acoustic navigation at mesoscale ranges. In Proceedings of the 2015 IEEE International Conference on Robotics and Automation (ICRA), Seattle, WA, USA, 26–30 May 2015; pp. 537–544. [[CrossRef](#)]
174. Hickey, H. One Year into the Mission, Autonomous Ocean Robots Set a Record in Survey of Antarctic Ice Shelf. Available online: <https://www.washington.edu/news/2019/01/23/one-year-into-their-mission-autonomous-ocean-robots-set-record-in-survey-of-antarctic-ice-shelf> (accessed on 18 March 2020).



© 2020 by the authors. Licensee MDPI, Basel, Switzerland. This article is an open access article distributed under the terms and conditions of the Creative Commons Attribution (CC BY) license (<http://creativecommons.org/licenses/by/4.0/>).

Copyright of Remote Sensing is the property of MDPI Publishing and its content may not be copied or emailed to multiple sites or posted to a listserv without the copyright holder's express written permission. However, users may print, download, or email articles for individual use.